Energy & Environmental Science

Cite this: *Energy Environ. Sci.*, 2012, **5**, 5884

www.rsc.org/ees

REVIEW

Na-ion batteries, recent advances and present challenges to become low cost energy storage systems

Verónica Palomares,[a] Paula Serras,[a] Irune Villaluenga,[a] Karina B. Hueso,[a] Javier Carretero-González[b] and Teófilo Rojo*[ab]

Received 28th September 2011, Accepted 19th December 2011
DOI: 10.1039/c2ee02781j

Energy production and storage have become key issues concerning our welfare in daily life. Present challenges for batteries are twofold. In the first place, the increasing demand for powering systems of portable electronic devices and zero-emission vehicles stimulates research towards high energy and high voltage systems. In the second place, low cost batteries are required in order to advance towards smart electric grids that integrate discontinuous energy flow from renewable sources, optimizing the performance of clean energy sources. Na-ion batteries can be the key for the second point, because of the huge availability of sodium, its low price and the similarity of both Li and Na insertion chemistries. In spite of the lower energy density and voltage of Na-ion based technologies, they can be focused on applications where the weight and footprint requirement is less drastic, such as electrical grid storage. Much work has to be done in the field of Na-ion in order to catch up with Li-ion technology. Cathodic and anodic materials must be optimized, and new electrolytes will be the key point for Na-ion success. This review will gather the up-to-date knowledge about Na-ion battery materials, with the aim of providing a wide view of the systems that have already been explored and a starting point for the new research on this battery technology.

1. Introduction

Energy conversion and storage have become key issues concerning our welfare in daily life. The urgent need for using renewable and cleaner energy sources, such as solar radiation, wind and waves, has brought about the problem of modulating energy sources that are variable in time and diffuse in space. These sources require storing the off-peak electricity and releasing the stored energy during the on-peak period, so that the efficiency, stability, and reliability of an electricity supply system can be significantly improved. The most appropriate form of energy storage in terms of energy density is chemical energy. For this purpose, batteries provide stored chemical energy with the ability to deliver it as electrical energy with high conversion efficiency and no gaseous exhaust. Therefore, of great interest are low-cost, safe, rechargeable batteries of adequate voltage, capacity, and rate capability.

Among the various available energy storage technologies, the Li-ion battery, which has conquered the portable electronic market, has become the prime candidate to power the next generation of electric vehicles and plug-in electric vehicles. Li-ion cells offer the largest energy density and output voltage of all rechargeable battery technologies in use. Moreover, Li-ion technology relies on a rich and versatile chemistry leading to

[a]*Departamento de Química Inorgánica, Universidad del País Vasco UPV/EHU, P.O. Box. 644, 48080 Bilbao, Spain. Fax: +34 946013500; Tel: +34 946012458*
[b]*CIC ENERGIGUNE, Parque Tecnológico de Álava, Albert Einstein 48, ED.CIC, 01510 Miñano, Spain. E-mail: trojo@cicenergigune.com; Tel: +34 945297108*

Broader context

In the present framework, it is undeniable that the world has to face energy challenges in a sustainable way. For this reason, and taking into account recent concerns about a possible lithium shortage with the spread of electric vehicles, it is urgent to search for alternative energy storage systems that could complement the existing Li-ion technology. For this purpose, Na-ion technology can be a suitable choice in terms of battery cost, safety and raw material abundance. Although these systems would be of lower energy density, they could be applied in static storage to buffer renewable energy. In order to be ready to introduce new alternative energy storage systems in the market, Na-ion knowledge must be deeply explored. This work claims to be a good starting point for this purpose.

a wide range of attractive electrode materials for both positive ($LiCoO_2$, $LiMn_2O_4$, $LiFePO_4$) and negative electrodes (C, Sn, Si, *etc.*).

This way, up till now, Li-ion batteries have attracted all the attention in energy storage, but recently, Na-based compounds have made a comeback because of controversial debates regarding the size of reserves and higher cost to obtain Li.[1] Of late, concerns have surfaced about the resource availability of lithium and hence future cost, in light of the projected orders-of-magnitude increase in lithium usage in batteries for low emission hybrid and electric vehicles (EV). While modest expansion of Li production can support 1 MM 40 kW h vehicle batteries, to meet a long-term target of 100 MM 40 kW h Li-based EV batteries per year a dramatic expansion of annual production will be necessary (more than one order of magnitude).[2] The issue is not insufficient lithium on a global scale, but what fraction can be used and still be economically effective.[3] Most untapped lithium reserves occur in remote or politically sensitive areas. Scale-up will require a long lead time, involve heavy capital investment in mining, and may require the extraction and processing of lower quality resources, which could drive extraction costs higher. Currently, high costs remain a critical barrier to the widespread scale-up of battery energy storage. With respect to the long-term "stock" goal of 1 billion 40 kWh vehicle batteries, the reserve base of several Li-based materials is sufficient, but near the limit of what is available. Indeed, if such a path is pursued, Li recycling will be necessary (see ref. 2). While the debate over the feasibility and environmental impact of lithium carbonate production continues, sodium-based compounds are under consideration as options for large scale energy storage coupled to renewable energy sources, for example. Expansion of battery research into alternative materials may accelerate the ability to work through both the scaling and cost challenges inherent in long-term planning for battery energy storage,[2]

Verónica Palomares

Verónica Palomares (1981, Bilbao) received her PhD in Chemistry from the University of the Basque Country (UPV/EHU) in 2009. During her PhD she worked on nanostructured cathodes for Li-ion batteries in collaboration with Cidetec-IK4. She has been a post-doctoral fellow at the University of the Basque Country, and nowadays is an associate professor at the UPV/EHU. She works in the field of new electrode materials for lithium and sodium ion batteries.

Irune Villaluenga

Irune Villaluenga (1982, Bilbao) received her PhD in Chemistry in 2010 from the University of the Basque Country (UPV/EHU) for research carried out at Tecnalia Research & Innovation. During her PhD she investigated TiO_2 nanoparticles and coatings for air and water purification and undertook internships at the University of Stockholm (Sweden) and the National Institute of Advanced Industrial Science and Technology (Japan). She is currently working as a researcher at the University of the Basque Country in the field of novel polymer electrolytes for sodium ion batteries.

Paula Serras

Paula Serras Malillos (1983, San Sebastian) is an Environmental Chemical Engineer from the Faculty of Engineering of Bilbao (2001–2006). She has been working in wastewater treatment area for almost four years in LEIA (Miñano, 2006–2007) and CEIT (San Sebastian, 2007–2010) research centers. At the moment she is a PhD student in the Department of Inorganic Chemistry at UPV/EHU and she is working in the field of new cathode materials for sodium ion batteries.

Karina B. Hueso

Karina Beatriz Hueso was born in Nevers, France. She received her PhD in Analytical Chemistry from the University of Salamanca (USAL, Spain) in 2010. During her PhD she spent two months at the Faculty of Science and the Environment at the University of Hull, United Kingdom. She has a multidisciplinary background in the fields of fluorimetry, biochemical, biopolymers and flow-injection analysis. After obtaining a master's degree in new materials from the University of the Basque Country (UPV-EHU, Spain) in 2011, she joined the Inorganic Chemistry department at UPV-EHU. Currently, her research interests focus on novel materials for sodium-ion batteries.

therefore it is imperative to seek low-cost alternatives that are not resource-limited.

The use of Na instead of Li in rocking chair batteries could mitigate the feasible shortage of lithium in an economic way, due to the unlimited sodium sources, the ease to recover it, and its lower price (Table 1). Moreover, for positive electrode materials sodium intercalation chemistry is very similar to Li, thus making it possible to use very similar compounds for both kinds of systems. Furthermore, if a rechargeable sodium-ion battery with good performance characteristics could be developed, it could have the advantage of using electrolyte systems of lower decomposition potential due to the higher half-reaction potential for sodium relative to lithium. This low voltage operation would make Na-ion cells cheaper, because water-based electrolytes could be used instead of organic ones. This alkali metal has already been successfully used in Na/S and Na/$NiCl_2$ Zebra cells.

It must be pointed out that electrochemical Na-ion cells will always fall short of meeting energy densities compared to Li-ion batteries. First, because equivalent weight of Na is higher than Li, and second because there are two competing factors regarding the formation of sodium-based intercalation compounds commonly employed as anode materials in "rocking chair" type batteries: one is the ionization potential and the other the size of the alkali metal. The ionization potential increases from 3.893 eV to 5.390 eV as we go from Cs to Li in the series of alkali metal elements in the periodic table. The lower the ionization potential, the more easily the electron transfers from the alkali metals to graphite for example, which is used as standard anode material. Consequently, the energy gain upon the charge transfer becomes smaller in the order of Cs > Rb > K > Na > Li. However, this picture looks inconsistent with what really happens with lithium intercalation. This fact can be explained by the smallness of the ionic diameter of Li. The ionic diameter decreases from 4 Å to 2 Å for the same series. Thus, Na-based cells will have difficulties competing with Li based cells in terms of energy density. However, they can be considered for use in applications where the weight and footprint requirement is less drastic, such as storage of off-peak and essentially fluctuating renewable energies, such as wind and solar farms. In spite of these considerations, there exists growing interest on Na-ion technology. Recent computational studies by Ceder *et al.* on voltage, stability and diffusion barrier of Na-ion and Li-ion materials indicate that Na-ion systems can be competitive with Li-ion systems.[5] In any case, Na-ion batteries would be interesting for very low cost systems for grid storage, which could make renewable energy a primary source of energy rather than just a supplemental one.

The search for commercially viable Na-ion batteries demands finding and optimizing new electrode materials and electrolytes, in order to get more economic, safer and long life batteries. One of the ways to get more economic systems would be searching for an aqueous electrolyte battery that would not need ultra-dry fabrication conditions and would not use higher cost organic electrolytes, such as sodium fluorinated salts. Another indirect saving could be the use of cheaper materials in the assembly of the battery, for example, the current collectors.

Table 1 Main characteristics of Na and Li materials

Characteristics	Na	Li
Price (for carbonates)[4]	0.07–0.37[a] € kg^{-1}	4.11–4.49[b] € kg^{-1}
Capacity density	1.16 A h g^{-1}	3.86 A h g^{-1}
Voltage *vs.* S.H.E.[c]	−2.7 V	−3.0 V
Ionic radius	0.98 Å	0.69 Å
Melting point	97.7 °C	180.5 °C

[a] Purity: 98.8–99.2% min. [b] Battery grade: 99.9%. [c] S.H.E.: Standard Hydrogen Electrode.

Javier Carretero-González

Javier Carretero González studied Chemistry at the Universidad Complutense. He obtained his PhD in 2009 working in polymer nanocomposites with Dr Miguel Angel Lopez Manchado at the Institute of Polymer Science and Technology. Javier joined the Nanotech Institute at the University of Texas at Dallas in 2008 with Professor Ray H. Baughman first as a PhD student and later as a research associate. At Nanotech he was working on multifunctional materials based on carbon nanotubes, graphene nanoribbons, electrochemical capacitors as well as in the rational design of carbon nanotubes of unique type. Currently Javier is a postdoctoral researcher at CIC Energigune.

Teófilo Rojo

Teófilo Rojo received his PhD from the University of the Basque Country in 1981. He has spent various research periods at several European and American universities. Since 1992 he has been a Full Professor of Inorganic Chemistry at the UPV-EHU. His research has been focused on Solid State Chemistry and Materials Science. Since 2010 he is the Scientific Director of the CIC-Energigune and his research is focused on the study of materials for both lithium and non-lithium based batteries. He holds different positions in various scientific bodies in Spain, being the chairman of the Solid State Chemistry Group within the Spanish Royal Society during the last ten years.

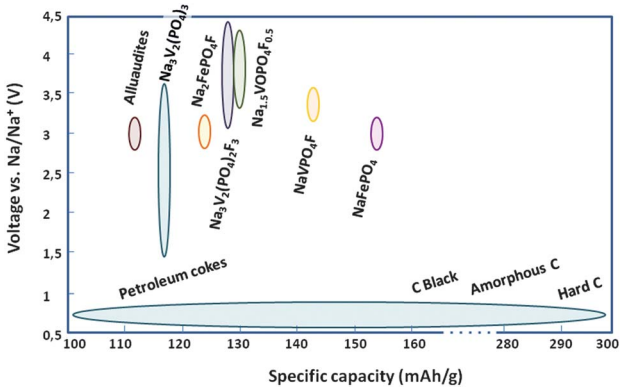

Fig. 1 Most important cathode and anode materials studied for their application in sodium ion batteries, represented by their specific capacity and operating voltage *versus* a sodium metal anode.

Fig. 1 depicts the most important cathodic and anodic materials for sodium-ion batteries, indicating their specific capacity and operating voltage.

As it can be seen, many materials have been proposed in the literature as possible cathodes for Na-ion batteries, whereas only some carbon-based anodes have been pointed out for this storage technology. This disparity can be observed in the different lengths of the cathode and anode sections of this work.

The best candidates to be cathodic materials in a Na-ion battery are phosphate based materials, because of their thermal stability and higher voltage due to the inductive effect. We can mention olivine $NaFePO_4$, with the highest theoretical specific capacity, $NaVPO_4F$, $Na_3V_2(PO_4)_2F_3$, Na_2FePO_4F and $Na_3V_2(PO_4)_3$. These phosphates require conductive coating and nanostructured morphology in order to improve their electrochemical performance.

Among the possible electrolytes, the use of both solid polymer systems and aqueous electrolytes is studied by many researchers. In particular, gel polymer electrolytes are prepared by combining a polymer matrix with an ionic liquid and/or nanoparticles and have a unique hybrid structure. Moreover, gel polymer electrolytes possess cohesive properties of solids and diffusive properties of liquids simultaneously. On the other hand, aqueous electrolytes such as Na-based aqueous electrolyte could be made for a lower cost. Specifically, Na_2SO_4, $NaNO_3$, $NaClO_4$, Na_3PO_4, Na_2CO_3, and NaOH solutions could be used to generate aqueous electrolytes.

In the case of anodic materials, the use of metallic sodium is not advisable because of dendrite formation and interface aging problems. Moreover, alternative anode materials must be searched in order to make aqueous Na-ion cells. This work gathers the most representative materials that have been tested in Na-ion cells, or that could be good candidates to be used in Na-ion technology.

2. Cathodic materials

2.1. Oxides

Research on positive electrodes for lithium and sodium electrochemical cells was first focused on several sodium–cobalt and sodium–manganese oxides.

Na_xCoO_2 bronzes have been tested as cathodes for Na polymer electrolyte cells. In Na_xCoO_2 bronzes x may be varied in the range $0.4 < x < 1$. These compounds are layered oxides with the sequence OMOAOMOA…, where O = oxygen, M = Co and A = Na. Within the composition range $0.5 < x < 1$, up to four phases have been identified in which the sodium coordination is either octahedral or trigonal prismatic.[6–9,56] In the nomenclature used to distinguish these phases, O and P represent octahedral or trigonal prismatic coordination of the sodium ions and 3 or 2 represents the number of distinguishable sodium layers. This way, O3, O′3, P3 and P2 phases are comprised in the mentioned x range. Although all these four phases have been shown to react reversibly *versus* sodium insertion, P2 bronze offers better cycle life and better energy efficiency,[10] thus it was studied more deeply.

Doeff *et al.* prepared sodium electrochemical cells using $P(EO)_8NaCF_3SO_3$ (polyethylene oxide sodium trifluoromethanesulfonate) as electrolyte and metallic sodium as anode. These cells showed an open circuit potential of about 2.8 V when operated at 90–100 °C.[11] Discharge of the P2-Na_xCoO_2 material led to sloping curves with several voltage steps due to ordering transitions of the Na ions between the layers (Fig. 2). Thus, cationic distribution in P2-Na_xCoO_2 phase changes with sodium content, leading to diverse Na^+/vacancy ordered distributions for definite sodium concentrations. Registered cationic exchange was of 0.5–0.6, which would correspond to *ca.* 141 mA h g^{-1}. Cyclability limitations associated with cathodic material were observed.

The crystal structure of the sodium cobalt oxide P2-Na_xCoO_2 phase during cycling *versus* Na/Na^+ has recently been published by Delmas *et al.* It showed a multistep voltage–composition curve with several reversible biphasic and single-phase domains from 2 to 3.8 V.[12]

On the other hand, Na insertion and extraction into and from P2-$Na_{2/3}[Ni_{1/3}Mn_{2/3}]O_2$ phase have been studied by Lu and Dahn.[13] All the sodium can be reversibly extracted from the phase, unlike its Li analog that only extracts 1/3 of the Li ions. This way a specific capacity of 161 mA h g^{-1} was achieved, very close to the theoretical one, of 173 mA h g^{-1}. Several voltage *plateaux* were observed from 3 to 4.1 V *vs.* Na/Na^+.

Because of the complexity of the electrochemical behavior of P2-Na_xCoO_2 and P2-$Na_{2/3}[Ni_{1/3}Mn_{2/3}]O_2$ systems, exhibiting

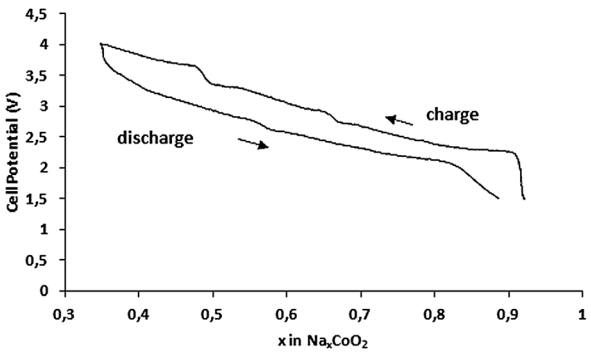

Fig. 2 Cell potentials *vs.* x for Na_xCoO_2 in a cell with a sodium anode and a $P(EO)_8NaCF_3SO_3$ electrolyte at 90 °C. The current density was 0.5 mA cm^{-2}. Reproduced by permission of The Electrochemical Society from ref. 11.

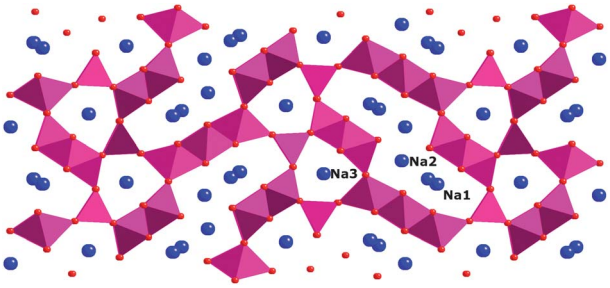

Fig. 3 Structure of $Na_{0.44}MnO_2$ perpendicular to the *ab* plane.

plateaux and sloping zones at different voltages, these materials cannot be considered as appropriate electrodes for Na-ion batteries.

Among the small number of oxide materials of potential interest identified as possible candidates to be used in secondary sodium battery applications, $Na_{0.44}MnO_2$ is particularly attractive because of its crystal structure forming suitable large-size tunnels for sodium incorporation.[14] Manganese oxides form a very rich and versatile structural family enlisting materials having either 1D, 2D, or 3D type tunnel structures.[15] $Na_{0.44}MnO_2$ crystallizes in an orthorhombic lattice cell with *Pbam* space group (Fig. 3). The manganese ions are located in two different environments: all Mn^{IV+} ions and half of the Mn^{III+} cations are in octahedral sites (MnO_6), while the other Mn^{III+} are gathered in a square-pyramidal environment (MnO_5). The latter forms edge-linked chains linked to two double and one triple octahedral chain(s) by the vertices, leading to the formation of two types of tunnels. Two sodium sites (referenced as Na1 and Na2) are situated in large S-shaped tunnels, while another site (Na3) is found in smaller tunnels. According to this structure, the *c* direction is the main path for sodium diffusion. The entitled $Na_{0.44}$/Mn ratio corresponds to a filling of the Na3 sites, whereas the S-shaped tunnels are only half filled.

The sodium manganese bronze Na_xMnO_2 phase was first studied by Doeff *et al.* as cathode material for both sodium and lithium secondary batteries. A reversible intercalation of 0.6 Na^+ or Li^+ ions per manganese, 160–180 mA h g^{-1} specific capacity, was observed at moderate current densities and 85 °C in a solid polymer electrolyte battery.[16]

Structural *in situ* study of $Na_{0.44}MnO_2$/C composite electrodes in a Na-ion cell during cycling was performed by Tarascon *et al.*[17] Na content varied in the range 0.18–0.64 between 2 and 3.8 V *vs.* Na/Na^+. The potential–composition curve showed multi-transition processes, underlining the complexity of the insertion/deinsertion mechanism. The incremental capacity curve obtained in PITT (Potentiostatic Intermittent Titration Technique) mode indicates the presence of at least five biphasic transitions on narrow domains within the $0.22 \leq x \leq 0.66$ composition range (Fig. 4).

Specific capacity of 140 mA h g^{-1} was achieved at very low currents (*C*/200). Capacity retention of this oxide at *C*/10 was not good because half of the capacity was only retained after 50 cycles. When this material was cycled faster than *C*/20, a drastic decrease in the capacity was noticed, demonstrating kinetic limitations. Further work would be needed in order to limit the self-discharge effect and the short cycling life, either by coating of the particles or *via* cationic substitution.

The sodium intercalation compound $Na_{0.44}MnO_2$ has been revisited by Whitacre as a potential positive electrode in an aqueous electrolyte hybrid energy storage device.[18] Activated carbon was chosen as anode material, and 1 M Na_2SO_4 solution was used as electrolyte. This hybrid system was cycled through a 0.6 V range from $Na_{0.44}MnO_2$ to $Na_{0.22}MnO_2$, showing a specific capacity of 45 mA h g^{-1} (ref. 19) (Fig. 5). Cathodic material demonstrated to be fully stable in an aqueous environment. The electrochemical device demonstrated very good cyclability for 1000 cycles. The discharge capacity profile shown consists of a sloping line with very small *pseudo plateaux*, making it less appealing to battery applications.

A recent publication addresses NaV_6O_{15} nanorods as a possible cathodic material for sodium-based batteries.[20] This phase has been previously used in a lithium-ion battery, and it exhibited stable and reversible lithium-ion insertion/deinsertion with a 328 mA h g^{-1} specific capacity value.[21] Its structure consists of a $(V_2O_5)_x$ framework constructed by the VO_5 pyramid

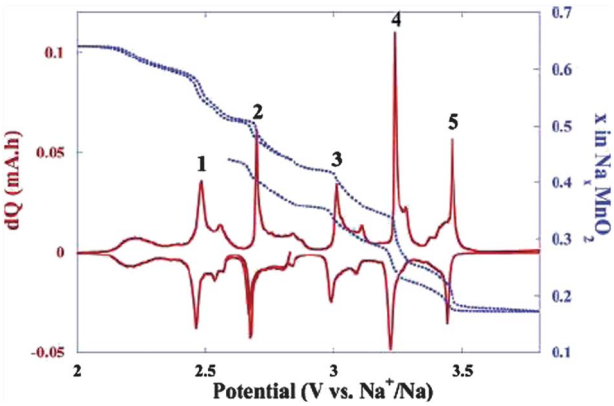

Fig. 4 PITT curve of a $Na_{0.44}MnO_2$/C composite electrode starting at reduction and corresponding incremental capacity curve. Reprinted with permission from: F. Sauvage, L. Laffont, J.-M. Tarascon, and E. Baudrin, *Inorganic Chemistry*, 2007, **46**, 3289–3294, Copyright 2007 American Chemical Society.

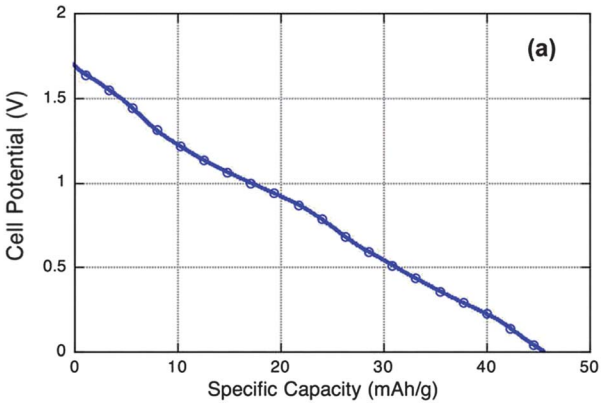

Fig. 5 Discharge profile of a $Na_{0.44}MnO_2$/activated carbon cell at *C*/8. Reprinted from: J. F. Whitacre, A. Tevar and S. Sharma, $Na_4Mn_9O_{18}$ as a positive electrode material for an aqueous electrolyte sodium-ion energy storage device, *Electrochemistry Communications*, **12**, 463–466, Copyright 2010, with permission from Elsevier.

and VO_6 octahedra. This framework possesses tunnels along the *b* axis, where Na ions are aligned.[22,23] NaV_6O_{15} nanorods aligned in the *c* direction showed a charge/discharge *plateau* at approximately 2.5 V *vs.* Na/Na^+, and a specific capacity value of 60 mA h g^{-1} at a medium cycling rate between 1.5 and 4 V. The need for controlling the cut-off potential window and current rate to get good specific capacity values and improved cycling stability makes it necessary to look for new ways of improving its electrochemical performance.

2.2. Transition metal fluorides

Fluoride-based cathode materials have also been proposed as cathodic materials for both Li and Na-ion batteries with the aim of overcoming the theoretical specific capacity limit of polyanionic cathodes. This way, $NaMF_3$ (M = Fe, Mn, V and Ni) type compounds have been prepared, with specific capacities ranging from 30 to 170 mA h g^{-1}.[24,25] Great polarization has also been observed for this family of compounds. Thus, further development is needed in order to make these compounds suitable cathodes for Na-ion batteries.

2.3. Phosphates

Framework materials based on the phosphate polyanion have recently been identified as potential electroactive materials for sodium metal and sodium ion battery applications. The metal phosphates based on either the olivine or NASICON structures appear to hold particular promise. It is the strong inductive effect of the PO_4^{3-} polyanion that moderates the energetics of the transition metal redox couple to generate relatively high operating potentials for these compounds.[26]

Table 2 displays some compounds that could be useful as cathodes in Na-ion batteries with their theoretical specific capacities.

2.3.1. Olivine $NaFePO_4$. The material with highest theoretical specific capacity is olivine $NaFePO_4$, with 154 mA h g^{-1}. This phase has not been deeply studied, as in the case of $LiFePO_4$, due to the difficulty to get it directly by standard routes. The most stable polymorph of $NaFePO_4$ is maricite, which is structurally analogous to $LiFePO_4$, but presents some important differences. In maricite, Na^+ cations occupy the 4(c) Wyckoff sites and the Fe^{2+} species are situated in 4(a) sites, while in olivine $LiFePO_4$ the Li^+ and Fe^{2+} ions occupy 4(a) and 4(c) sites, respectively. This is probably due to the larger ionic radius of Na^+ compared to that of Li^+.[27] This way, maricite presents one-dimensional, edge-sharing FeO_6 octahedra and no cationic channels, thus hindering

Table 2 Main phosphate phases that can be used as positive electrode material in Na-ion batteries and their theoretical specific capacity

Compound	e^- transfer	Theroretical capacity/mA h g^{-1}
$NaFePO_4$ (olivine)	1	154
$NaVPO_4F$	1	143
$Na_3V_2(PO_4)_2F_3$	2	128
$Na_{1.5}VOPO_4F_{0.5}$	1	130
Na_2FePO_4F	1	124
$Na_3V_2(PO_4)_3$	2	118
$NaFe_2Mn(PO_4)_3$	2	108

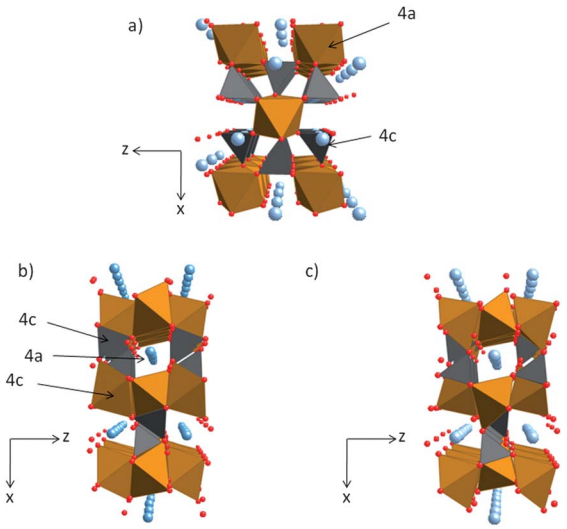

Fig. 6 Structure of (a) maricite $NaFePO_4$, (b) olivine $LiFePO_4$, and (c) olivine $NaFePO_4$. 4(a) and 4(c) crystallographic sites are marked.

cation exchange. Fig. 6 shows the crystallographic structure of the three compounds.

Recent preparation of the olivine $NaFePO_4$ and $Na_{0.7}FePO_4$ phases has been reported,[28] demonstrating reversible insertion and extraction of Na into olivine $FePO_4$ at 2.8 V. The preparation process involves two steps: first, chemical oxidation of $LiFePO_4$ to heterosite $FePO_4$ by using NO_2BF_4 in acetonitrile[29] or bromine dissolved in water,[10,30] and second, electrochemical Na insertion by using $FePO_4$ as the positive electrode and metallic Na foil as anode. A discontinuity in the potential–composition curve has been detected in the vicinity of $Na_{0.65}FePO_4$, both on discharge and on charge (Fig. 7, point B). This discontinuity corresponds to an electrochemical biphasic process involving a $Na_{0.7}FePO_4$ phase in equilibrium with $FePO_4$, as confirmed by *ex situ* X-ray diffraction diagrams. The occurrence of an intermediate phase while cycling in the case of sodium, whereas intermediate compositions for lithium iron phosphate were only characterized under special conditions,[31] illustrates the increasing interaction of sodium ions compared to lithium ones with the host structure. A similar behavior is observed by comparing the number of phases obtained in the Li_xCoO_2[32] and Na_xCoO_2 systems.[33]

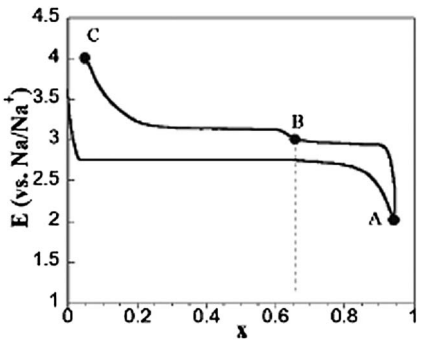

Fig. 7 Electrochemical curve for the synthesis of $NaFePO_4$ and $Na_{0.7}FePO_4$ in PITT mode. Reprinted with permission from: P. Moreau, D. Guyomard, J. Gaubicher and F. Boucher, *Chemistry of Materials*, 2010, **22**, 4126–4128, Copyright 2011 American Chemical Society.

A 147 mA h g^{-1} specific capacity has been obtained by Zaghib *et al.* in the first discharge of an electrochemically synthesized $NaFePO_4$ at 60 °C and *C*/24 rate (see ref. 30), but poor reversibility has been achieved by the moment (50.6 mA h g^{-1} in the second cycle). Moreau *et al.* could cycle reversibly 0.9 Na in the first charge/discharge cycle (139 mA h g^{-1}), but the cycle life of the produced material was not investigated. Much more work has to be performed with this material in order to develop a high capacity olivine Na-based cathodic material.

The research on olivine structure materials for Na-ion batteries has been extended to $Na[Mn_{1-x}M_x]PO_4$ (M = Fe, Ca, Mg) by Nazar *et al.*[34] A new method based on topochemical synthesis has demonstrated to be useful to prepare different sodium metal olivines from $NH_4MPO_4 \cdot H_2O$ precursor. Preliminary galvanostatic tests at low cycling rate in Na cells indicated that electrochemical reaction takes place in a single-phase, with a sloping voltage profile. However, this point must be confirmed, because kinetic limitations may induce the sloping voltage curve.

2.3.2. Sodium fluorophosphates. In the quest for new cathode materials, some sodium-based cathode materials have recently emerged as a new choice. A series of sodium fluorophosphates, for example, $NaVPO_4F$, $Na_3V_2(PO_4)_2F_3$, $Na_{1.5}VOPO_4F_{0.5}$ and Na_2FePO_4F, have shown to be promising candidates to be considered. Recent works have demonstrated that these cathode materials exhibit electrochemical behavior similar to that of the conventional lithium-based cathode materials.

2.3.2.1. Sodium vanadium fluorophosphates. The sodium vanadium fluorophosphates, involving $NaVPO_4F$, $Na_3V_2(PO_4)_2F_3$ and $Na_{1.5}VOPO_4F_{0.5}$, have attracted considerable interest due to the low-cost raw materials, safe applications and high working potentials.

$NaVPO_4F$ was first proposed by Barker *et al.*, who described it as a tetragonal symmetry structure (space group *I*4/*mmm*)[35] related to that found for the sodium aluminium fluorophosphate (α-$Na_3Al_2(PO_4)_2F_3$)[36] (Fig. 8). It is believed that this compound represents one of the first examples of fluorophosphate-based compounds that have been recognized as alkali ion insertion hosts. Indeed, this phase has been identified as a potential electroactive material for novel sodium ion applications.

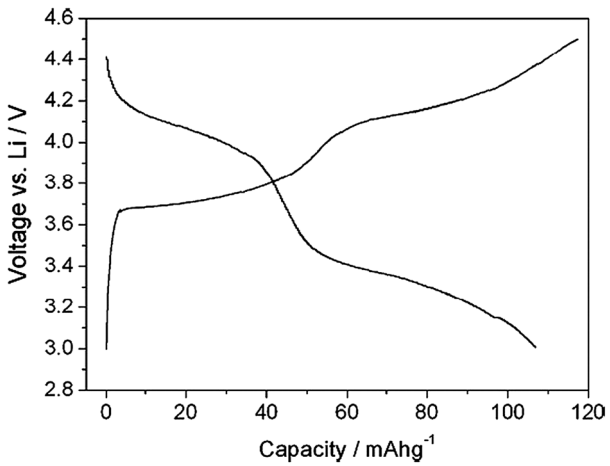

Fig. 8 First charge/discharge curves of the tetragonal $NaVPO_4F$ *vs.* Li/Li^+ at *C*/4 rate in the voltage range of 3.0–4.5 V in a hybrid lithium ion battery (from ref. 37). Reprinted from: J. Zhao, J. He, X. Ding, J. Zhou, Y. Ma, S. Wu and R. Huang, A novel sol–gel synthesis route to $NaVPO_4F$ as cathode material for hybrid lithium ion batteries, *Journal of Power Sources*, **195**, 6854–6859, Copyright 2010, with permission from Elsevier.

This compound has been electrochemically tested *vs.* metallic lithium and hard carbon anodes. Galvanostatic cycling of the $NaVPO_4F$ phase *vs.* Li/Li^+ between 3 and 4.5 V at *C*/4 rate revealed a 117 and 107 mA h g^{-1} charge and discharge specific capacity, respectively (Fig. 8). Repeated cycling at this rate provoked a discharge capacity fade of about 10% after 100 cycles. Thus, the mixed Li^+/Na^+ insertion reactions did not lead to unfavorable influence on the long-term cycling stability.[37]

A similar hybrid-ion cell made by Barker *et al.*[38] displayed a 110 mA h g^{-1} reversible specific capacity at a low rate. Cycle life tests at *C*/5 demonstrated outstanding insertion stability, characterized by reversibility of the alkali metal insertion reaction over an extended cycling regimen of 400 cycles (Fig. 9).

Galvanostatic cycling of the same phase in a Na-ion cell, *i.e. vs.* a hard carbon anode with a sodium electrolyte, at 23 °C and *C*/10 rate between 2.5 and 4.25 V, showed specific capacities of 79 and 82 mA h g^{-1} for the first discharge and second charge processes, respectively. Discharge capacity of this cell decayed to less than 50% of the initial one after 30 cycles (see ref. 45).

Concerning $NaVPO_4F$ compound, even if very good cyclability results have been observed in hybrid $Li//NaVPO_4F$ cells, improvements are already needed in Na-ion cells.

On the other hand, Zhao *et al.* (see ref. 37), Zhuo *et al.*[39] and Liu *et al.*[40] reported another interesting $NaVPO_4F$ phase as a monoclinic crystal with a space group of *C*2/*c*, which is in good agreement with the related $Na_3Al_2(PO_4)_2F_2$ phase. The structure of this material is described as made up of two $[PO_4]$ tetrahedra that share two corner-oxygen atoms with two different $[VO_4F_2]$ octahedra.

Zhao *et al.* (see ref. 37) described the formation of this $NaVPO_4F$ polymorph when using the sol–gel synthesis method and subsequent firing at 700 °C, whereas the tetragonal phase was formed at 750 °C.

Electrochemical tests of this monoclinic polymorph have only been carried out on doped samples, such as $NaV_{1-x}Al_xPO_4F$ and $NaV_{1-x}Cr_xPO_4F$ (see ref. 39 and 40). Specific capacity values

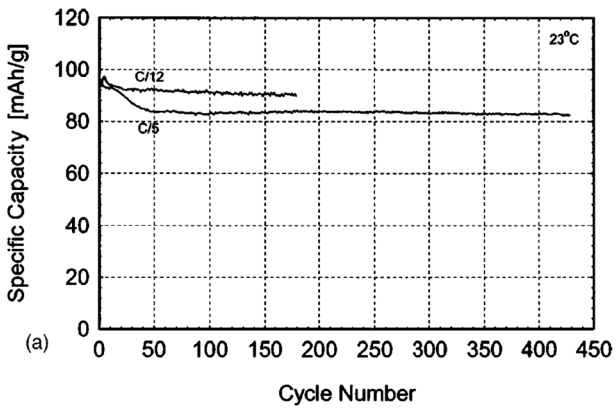

Fig. 9 Cyclability of $Li//NaVPO_4F$ cells cycled between 3.00 and 4.50 V at *C*/12 and *C*/5 rates. Reproduced by permission of The Electrochemical Society from ref. 38.

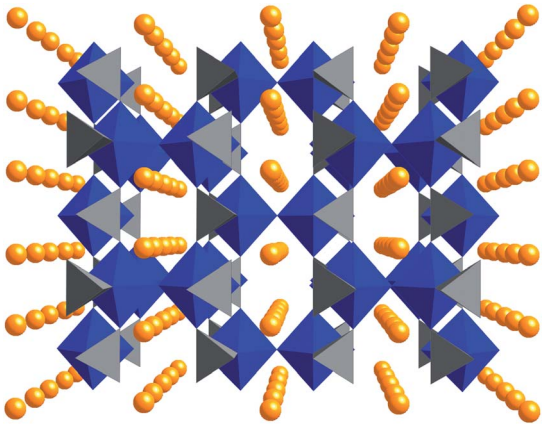

Fig. 10 Crystal structure of $Na_{1.5}VOPO_4F_{0.5}$. Polyhedral representation, spheres: disordered Na atoms (from ref. 41).

obtained in Na cells were around 80 mA h g^{-1}, and cycling performance of both samples was improved with doping.

The second vanadium fluorophosphate is the previously mentioned $Na_{1.5}VOPO_4F_{0.5}$. Its space group is *I*4/*mmm*, and it is formed by layers of alternating [VO_5F] octahedra and [PO_4] tetrahedra sharing O vertices parallel to the *ab* plane (Fig. 10). Along the *c* direction the V octahedra are joined pairwise through common F vertices in the inversion centres. The sixth O vertex of the V octahedron is the terminal oxo ligand of a vanadyl group. Thus, the structure is described by a mixed paraframework of octahedra and tetrahedra $\{V_2O_2F[PO_4]_2\}_{\infty\infty\infty}$ with disordered Na atoms in the interstices.[41] Crystal structure, electronic structure and magnetic behavior of the $Na_{1.5}VOPO_4F_{0.5}$ phase have been recently reported by Tsirlin *et al.*[42]

Only one article that presents electrochemical measurements of $Na_{1.5}VOPO_4F_{0.5}$ has been found.[43] Sauvage *et al.* assembled a Na-cell with the following configuration: [Na//$NaClO_4$ 1 M PC//$Na_{1.5}VOPO_4F_{0.5}$–C (composite)]. The electrochemical curve of the cathodic material was studied in PITT mode, and the extraction–insertion of Na into the structure proceeded in two different steps at about 3.60 and 4.00 V *vs.* Na/Na^+ (Fig. 11). A

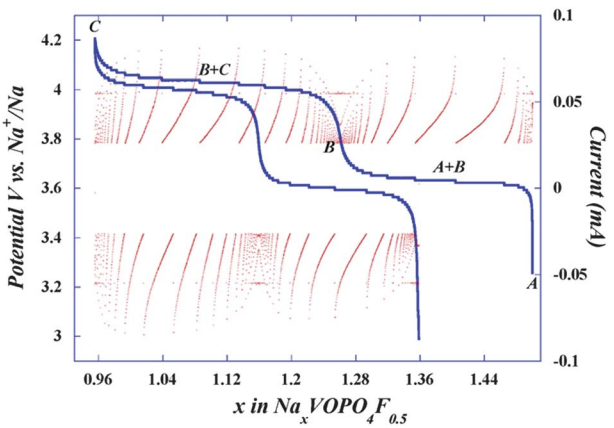

Fig. 11 Charge and discharge curve for $Na_{1.5}VOPO_4F_{0.5}$ *vs.* Na/Na^+ (from ref. 43). Reprinted from: F. Sauvage, E. Quarez, J. Tarascon and E. Baudrin, Crystal structure and electrochemical properties *vs.* Na of the sodium fluorophosphate $Na_{1.5}VOPO_4F_{0.5}$, *Solid State Sciences*, **8**, 1215–1221, Copyright 2006, with permission from Elsevier.

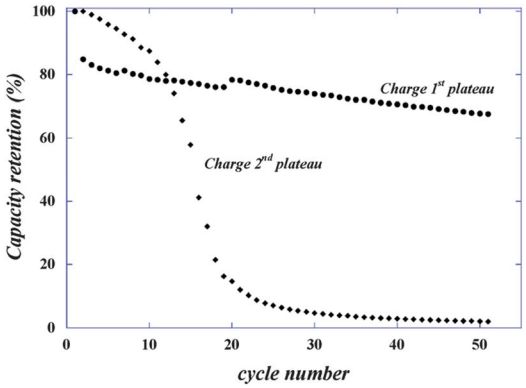

Fig. 12 Evolution of capacity retention of the 1st and 2nd *plateaux* recorded for $Na_{1.5}VOPO_4F_{0.5}$ in $NaClO_4$ 1 M/PC electrolyte over 50 cycles at *C*/20 rate (from ref. 43). Reprinted from: F. Sauvage, E. Quarez, J. Tarascon and E. Baudrin, Crystal structure and electrochemical properties *vs.* Na of the sodium fluorophosphate $Na_{1.5}VOPO_4F_{0.5}$, *Solid State Sciences*, **8**, 1215–1221, Copyright 2006, with permission from Elsevier.

specific capacity of 87 mA h g^{-1} was obtained by galvanostatic cycling of the material at *C*/20, which is below the theoretical one.

On the other hand, as it can be seen in Fig. 12, the lower voltage *plateau* process showed a sustained reversibility over 50 cycles, in contrast with a poor one for the high voltage process. This capacity fading was associated with a cell polarization increase that could be consistent with the formation of a surface layer resulting from electrolyte degradation at the surface of the materials.

Finally, the $Na_3V_2(PO_4)_2F_3$ phase has a tetragonal crystal structure with a space group of $P4_2/mnm$ (Fig. 13).[44] Structural analyses show that the crystal structure is consistent with the sodium aluminium fluorophosphate (α-$Na_3Al_2(PO_4)_2F_3$), which was put forward by Le Meins (see ref. 36).

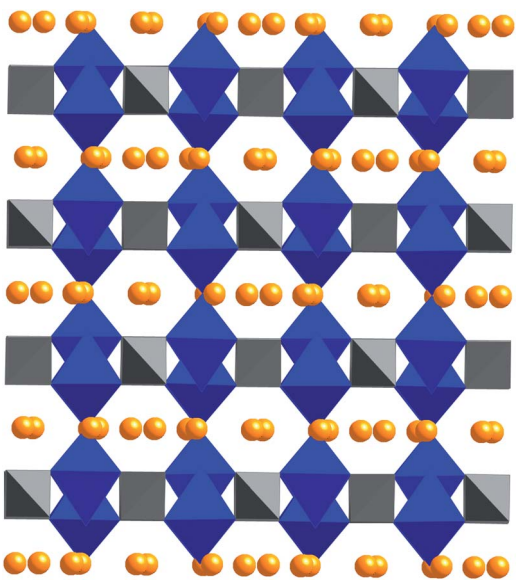

Fig. 13 Structural representation of $Na_3V_2(PO_4)_2F_3$ projected along the *a* direction.

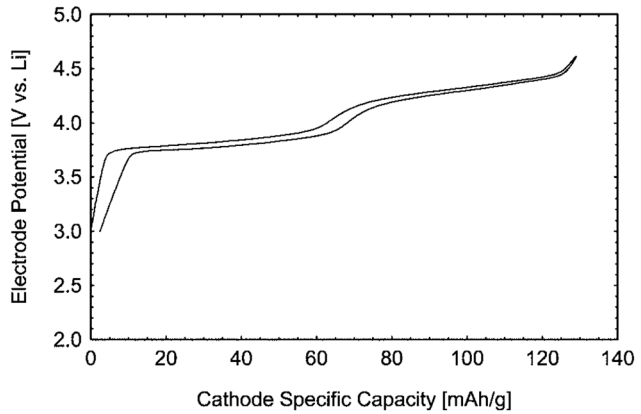

Fig. 14 $Na_3V_2(PO_4)_2F_3$ *vs.* Li/Li^+. Reproduced by permission of The Electrochemical Society from ref. 45.

Gover *et al.* demonstrated the reversible cycling of two alkali ions per formula unit for this compound in the 3–4.6 V potential range *vs.* a Li anode[45] (Fig. 14). Although an additional voltage *plateau* was present at around 4.9 V *vs.* Li, only a small percentage of the associated oxidation charge was found to be reversible. This observation may be consistent with electrolyte decomposition rather than some inherent active material limitation. The associated specific capacity at *C*/20 was around 120 mA h g^{-1}, at an average discharge voltage of around 4.1 V.

The stability of the insertion–extraction reactions was confirmed by long term cycling experiments at *C*/15 and *C*/7, which demonstrated low capacity fade over the initial 220 cycles.

Barker *et al.* carried out an interesting study by using $Na_3V_2(PO_4)_2F_3$ *vs.* a graphite anode with a $LiPF_6$ based electrolyte. The volume of electrolyte used was carefully controlled, so as to allow charging of the graphite active material to an approximate utilization limit of 300 mA h g^{-1} of $Li_{0.81}C_6$. During the initial charge process, sodium ions were extracted from the fluorophosphate cathode, while lithium ions from the electrolyte were intercalated into the graphite anode, forming a lithium-based solid electrolyte interphase (SEI) passivation layer on the carbon anode. Specific capacity data collected at *C*/2 and 2*C* charge–discharge rates showed reversible capacities in the range of 115–120 mA h g^{-1} (Fig. 15). The minor decrease in discharge capacity recorded at the two discharge rates is indicative of the insertion stability of this battery configuration (see ref. 45).

A recent article by Jiang *et al.* proved that the electrochemical insertion mechanism in a $Li//LiPF_6$ (EC/DMC)$//Na_3V_2(PO_4)_2F_3$ cell gradually shifted from predominant Na^+ insertion to Li^+ insertion in the initial cycles. Galvanostatic charge/discharge cycling of $Na_3V_2(PO_4)_2F_3$ carried out in the 3–4.5 V potential region at *C*/10 showed a specific capacity value very close to the theoretical capacity, 128 mA h g^{-1} with quite good capacity retention.[46]

To conclude, it must be remarked that Sauvage *et al.* (see ref. 43) questioned the stoichiometry given by Barker for $NaVPO_4F$. In fact, they mentioned that structural data of only two compounds containing the same five elements (Na, V, P, O and F) could be found in the literature: $Na_3V_2(PO_4)_2F_3$ and $Na_{1.5}VOPO_4F_{0.5}$. Up till now, to our knowledge, no structural data have been reported for the $NaVPO_4F$ phase.

2.3.2.2. Sodium iron fluorophosphates. Na_2FePO_4F has been tested as positive electrode material for Li-ion cells. This compound is isostructural with both Na_2FePO_4OH and Na_2CoPO_4F, and comprises bioctahedral $Fe_2O_7F_2$ units made of face-sharing FeO_4F_2 octahedra that are connected *via* bridging F atoms to form chains, and joined by PO_4 tetrahedra to form $[FePO_4F]$ infinite layers. The two Na cations located in the interlayer space possess facile two-dimensional migration pathways (Fig. 16).

This compound has been tested with a metallic lithium anode, exchanging rapidly one mobile Na for Li. This way, one sodium per formula is completely deintercalated upon charging of the material in a lithium electrochemical cell, showing a specific capacity of 124 mA h g^{-1} for 50 cycles at *C*/10 rate (see ref. 1). For this mixed cell, the (Na, Li)$FePO_4F$ compound has a theoretical specific capacity of 135 mA h g^{-1} and the electrochemical profile displays quasi-solid solution at room temperature.

The unit cell of the oxidized compound ($NaFePO_4F$) is only 3.7% smaller than that of Na_2FePO_4F, which makes this compound a low strain material. An intermediate $Na_{1.5}FePO_4F$ phase is obtained with lattice parameters intermediate between

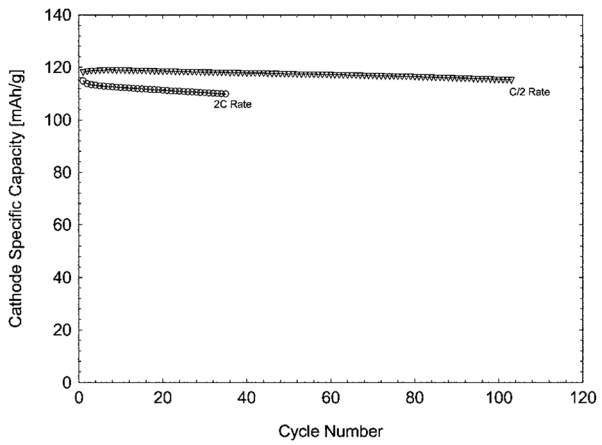

Fig. 15 Graphite$//LiPF_6$ (EC/DMC)$//Na_3V_2(PO_4)_2F_3$ cells between 3 and 4.6 V. Reproduced by permission of The Electrochemical Society from ref. 45.

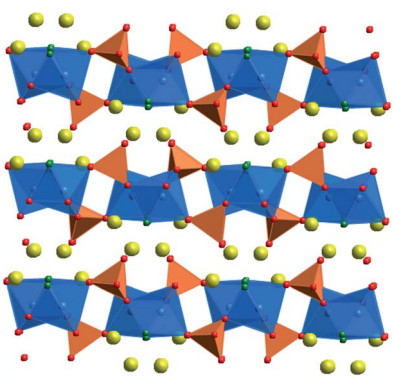

Fig. 16 Crystal structure of Na_2FePO_4F. The iron octahedra are plotted in blue, phosphate tetrahedra are shown in orange, fluorine atoms in green and Na ions in yellow.

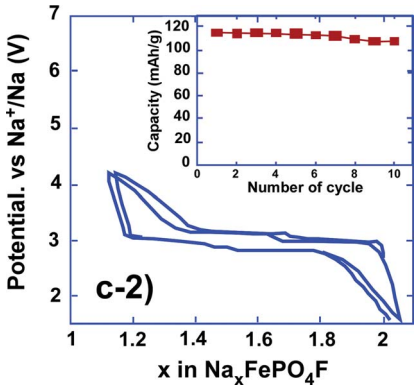

Fig. 17 Galvanostatic cycling *vs.* Na/Na$^+$ of the Na_2FePO_4F material synthesized by the ionothermal process at *C*/15 rate. Inset: Cyclability of Na_2FePO_4F. Reproduced by permission of The Electrochemical Society from ref. 47.

the two end members. Its structure undergoes a slight change in symmetry to a monoclinic unit cell (*P*2/*c*, $\beta = 91.22°$).

This compound has also been studied by Recham *et al.*[47] The ionothermal synthesis process consisted of using ionic liquids as both solvent and template to grow the desired phase at lower temperatures than those needed for solid state methods. This way, morphology could be controlled and 2.5 nm particles were obtained. Nanosized particles improved electrochemical performance slightly by showing better initial capacity, lower irreversible capacity, lower polarization and better capacity retention. These ionothermally synthesized compounds were tested both in Li and Na electrochemical cells. The discharge specific capacity in a sodium cell for this sample was over 100 mA h g^{-1} for 10 cycles. Electrochemical voltage profiles *versus* metallic sodium displayed a reversible two-*plateaux* behavior and lower potential, due to different alkali intercalation potentials within the same host material (Fig. 17).

2.3.2.3. Other sodium fluorophosphates. As in the case of Na_2FePO_4F, the Na_2MnPO_4F phase was also prepared by the ionothermal process. This phase is compositionally identical, but structurally distinct. It presents a tunnel structure formed by MnO_4F_2 entities where alkali cations are located (Fig. 18). In order to form these tunnels, manganese octahedra share only one common F vertex to form $Mn_2F_2O_8$ chains parallel to the *b*-axis of the monoclinic unit cell. These chains are linked by PO_4 tetrahedra in *a* and *c* directions and lead to tunnels for possible cationic Na transport.

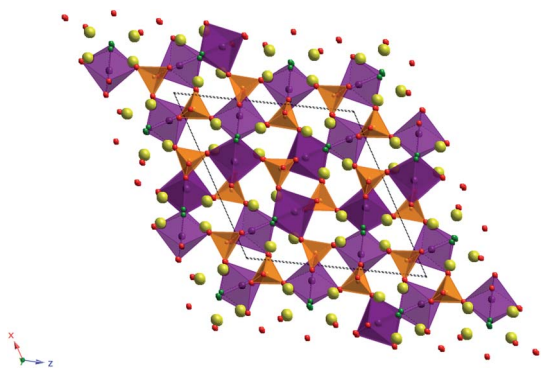

Fig. 18 Crystal structure of Na_2MnPO_4F. The manganese octahedra are plotted in purple, phosphate tetrahedra are shown in orange, fluorine atoms in green and Na ions in yellow.

Substitutions of Fe by Mn were also explored in the $Na_2Fe_{1-x}Mn_xPO_4F$ ($0 < x < 0.2$) series. Na_2MnPO_4F exhibited very poor electrochemical behavior despite the presence of an open pathway for alkali migration (see ref. 2). Electrochemical performance of substituted samples decreased with increasing the manganese content. Thus, Mn based species showed much worse performance, even in the same structure as the Fe-based compound.

On the other hand, in order to get higher voltage materials, the Na_2CoPO_4F phase was prepared by Ellis *et al.* (see ref. 3). This phase was structurally identical to the Fe analogue. Electrochemical tests *versus* a Li anode showed a good charging capacity (85% of the theoretical value) but a poor discharging capacity (25% of the theoretical value). This can be due to the high operation voltage of this material that cycles between 4.7 and 5 V *vs.* Li/Li$^+$. The use of a sodium anode would diminish the operation voltage and, thus, it would dim electrolyte degradation in order to provide longer cycle life and better specific capacity values.

Furthermore, Ellis *et al.* also prepared the Na_2NiPO_4F phase, which is isostructural to Na_2FePO_4F. An electrochemical cell which contained Na_2NiPO_4F as the positive electrode material did not show any electrochemical activity below 5 V, but it is expected that this compound has a Ni^{2+}/Ni^{3+} redox couple above 5 V, similar to that of other nickel phosphates such as $LiNiPO_4$[48] and Li_2NiPO_4F.[49] It is worth mentioning that this compound may also be used *versus* a sodium anode in order to investigate if the operation voltage is inside the electrolyte potential window.

Substitutional solid solutions such as $Na_2(Fe_{1-x}Co_x)PO_4F$ ($0 \leq x \leq 1$) and $Na_2(Fe_{1-x}Mg_x)PO_4F$ ($x < 0.15$) were also prepared (see ref. 3) but, in the first case, minimal reversibility was registered, and, in the second one, only slight improvements from the Na_2FePO_4F phase were observed.

2.3.3. $Na_3M_2(PO_4)_3$ NASICON framework compounds. NASICON (Na$^+$ superionic conductor)-related compounds have been shown to be promising cathode materials for lithium-ion batteries, exhibiting high Li$^+$ ion mobility and reasonable discharge capacities. The compounds with the highest ionic mobilities possess rhombohedral R-3 symmetry. Both Li and Na ions can be inserted into a series of compounds having a general formula $A_nM_2(XO_4)_3$ because they have a large lithium or sodium site based on a 3D framework. The $M_2(XO_4)_3$ scaffold is built of $(XO_4)_{n-}$ (X = Si^{4+}, P^{5+}, S^{6+}, Mo^{6+}, *etc.*) tetrahedral corner-linked to octahedral-site M^{m+} (M = transition metal). In this structure, alkali ions can occupy two different sites. At low alkali content ($x < 1$ in $A_xM_2(XO_4)_3$) an octahedral site, A(1), is selectively occupied (Fig. 19).[50] With $x > 1$, the alkali ions are randomly distributed among the A(1) and three 8-coordinate sites, A(2). This way, the open 3D nature of the structure allows easy migration of the alkali ions between A(1) and A(2).

The $Na_3V_2(PO_4)_3$ compound was used to prepare rhombohedral $Li_3V_2(PO_4)_3$ because monoclinic polymorph is obtained by direct synthesis of the Li phase. This way, rhombohedral

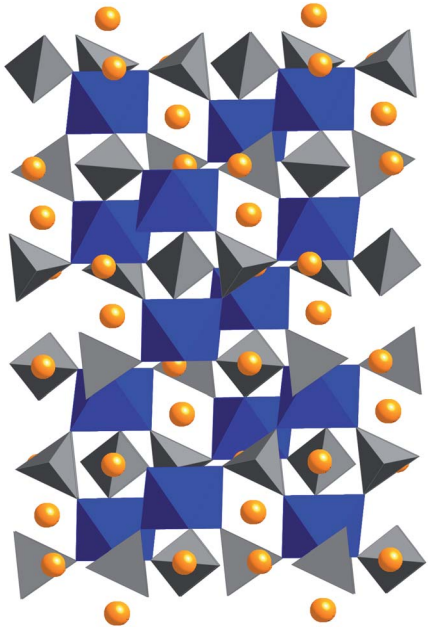

Fig. 19 Rhombohedral form of the NASICON structure.

$Li_3V_2(PO_4)_3$ was prepared by chemical oxidation of $Na_3V_2(PO_4)_3$ to $V_2(PO_4)_3$, followed by intercalation of Li,[51] or by ion exchange by stirring the Na phase in an aqueous solution of $LiNO_3$[52,53] or LiBr,[54] or LiCl in *n*-hexanol.[55] As obtained rhombohedral $Li_3V_2(PO_4)_3$ can extract two alkali cations/electrons between 3 and 4.5 V under *C*/10 conditions in a two-phase process with an equilibrium potential of 3.77 V (see ref. 52). Moreover, a mixed-alkali insertion NASICON $Li_2NaV_2(PO_4)_3$ cathode produced a discharge capacity of 96 mA h g^{-1} at 0.50 mA cm^{-2}, with a 10% capacity fade through the first 50 cycles (see ref. 53).

Rhombohedral NASICON form of $Na_3V_2(PO_4)_3$ was firstly tested as cathodic material *versus* metallic sodium by Yamaki *et al.*[56] showing reversible sodium insertion up to 0.8 Na^+ and subsequent extraction up to 2.6 Na^+ ions. This way, the initial phase was cycled from $x = 1.2$ to $x = 3.8$ in $Na_xV_2(PO_4)_3$. Two *plateaux* were observed for this composition range: one at 1.5 V *vs.* Na/Na^+ when $3 \leq x \leq 3.8$ and the other one when $1.2 \leq x \leq 3$. In the same work, the $Na_3Fe_2(PO_4)_3$ compound was also tested as positive electrode material *versus* sodium, but it only showed a *plateau* around 2.5 V, and a discharge specific capacity of 45 mA h g^{-1} for the first cycle.

In a similar way, $Na_3Fe_2(PO_4)_3$ has also been used to prepare rhombohedral $Li_3Fe_2(PO_4)_3$ by ion exchange, using a concentrated aqueous solution of $LiNO_3$ at 40 °C. The as prepared material exhibited a long, flat *plateau* at around 2.7 V *vs.* Li/Li^+ which corresponded to 1.6 Li^+ ion insertion per formula unit.[57]

Fig. 20 shows the reversible gravimetric energy density for the first cycle of different electrochemical systems, calculated from experimental data (see ref. 56). As it can be seen $Na/Na_3V_2(PO_4)_3$ provides more energy than other related compounds.

In the case of the vanadium NASICON the existence of two voltage *plateaux* at 1.6 and 3.4 V *vs.* Na/Na^+ allows using this phase not only as cathode but also as anode in a symmetric cell depending on the voltage window used. This kind of cell has been

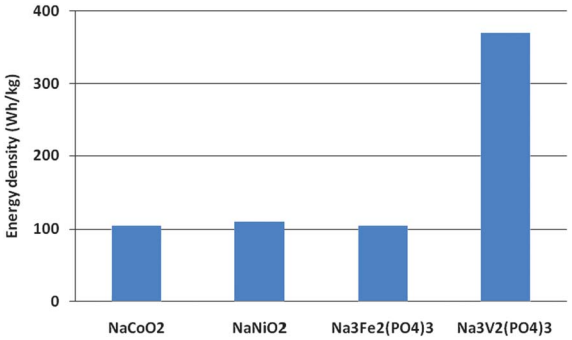

Fig. 20 Reversible gravimetric energy density for the first cycle of different cathode materials in a sodium battery with liquid organic electrolytes at room temperature (data from ref. 56).

built by Yamaki *et al.*[58] and the key cell reactions in the considered symmetric cells can be described as follows:(Anode):

$$Na_3V_2^{3+}(PO_4)_3 + xNa^+ + xe^- \leftrightarrows Na_{3+x}V_{2-x}^{3+}V_x^{2+}(PO_4)_3 \quad (1)$$

(Cathode):

$$Na_3V_2^{3+}(PO_4)_3 \leftrightarrows Na_{3-x}V_{2-x}^{3+}V_x^{4+}(PO_4)_3 + xNa^+ + xe^- \quad (2)$$

(Overall cell reaction):

$$Na_3V_2^{3+}(PO_4)_3 \leftrightarrows Na_{3+x}V_{2-x}^{3+}V_x^{2+}(PO_4)_3 + Na_{3-x}V_{2-x}^{3+}V_x^{4+}(PO_4)_3 \quad (3)$$

First, the $Na_3V_2(PO_4)_3$ material was tested *vs.* a metallic sodium anode. As it can be seen in Fig. 21, the electrochemical profile of the material showed a clear *plateau* at about 3.4 V which corresponded to the extraction of almost 1.7 atom of sodium associated with the V^{4+}/V^{3+} redox reaction, and a lower voltage *plateau* associated with the V^{3+}/V^{2+} couple around 1.6–1 V.

Symmetric $Na_3V_2(PO_4)_3$//1 M $NaClO_4$/PC//$Na_3V_2(PO_4)_3$ cells were found to work as reversible sodium ion batteries with coulombic efficiency of 75% for the first cycle. To improve the safety, a non-flammable electrolyte based on $EMIBF_4$ ionic

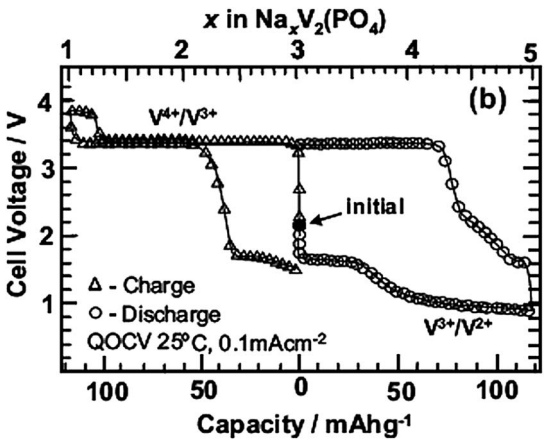

Fig. 21 Electrochemical charge–discharge curves for the $Na_3V_2(PO_4)_3$// 1 M $NaClO_4$/PC//Na cells at room temperature. Reproduced by permission of The Electrochemical Society from ref. 58.

liquid (1-ethyl-3-methyl imidazolium tetrafluoroborate) was used instead of explosive organic solvents. The substitution of the organic electrolyte by the ionic liquid-based one in the examined symmetric cell resulted in the decrease of the first discharge capacity and rate capability at high current densities. However, the ionic liquid-based cell exhibited better cycling performance due to the lower reactivity of the ionic liquid used.

Compounds based on the NASICON framework are remarkable because of their compatibility with aqueous electrolytes. This fact makes these phases very interesting from the economical point of view, because an aqueous electrolyte-based battery would contribute to diminish production costs and, in combination with sodium affordable price, it would produce a low cost battery.

2.3.4. Alluaudite framework compounds. Within the set of phosphate compounds that exhibit framework structures built up from both (MO_n) polyhedral and $(PO_4)^{3-}$ tetrahedral polyanions, alluaudite type phases were first pointed out as Li insertion hosts by T.J. Richardson.[59] This group of compounds has the general formula $X^1X^2M^1M_2^2(PO_4)_3$, where X^1 and X^2 are cations residing in different sites in *c*-axis oriented tunnels formed by chains of edge-shared MO_6 octahedra linked by tetrahedral PO_4 units (Fig. 22). $NaFe_3(PO_4)_3$ and $Li_xNa_{2-x}FeMn_2(PO_4)_3$ alluaudite compounds were prepared, but obtained reversible specific capacities were very low and significant hysteresis was observed between charge and discharge processes.

On the other hand, Delmas *et al.* have recently pointed out $NaMnFe_2(PO_4)_3$ alluaudite type phases as feasible polyanion-based insertion hosts.[60] The solid state synthesis method led to 1–3 μm sized particles of the desired material. When $NaMnFe_2(PO_4)_3$ was tested as the positive electrode in lithium cells, up to 0.2 Na^+ ions per formula unit could be extracted during the first charge with an average voltage around 3.2 V, and about 1.8 and 1.4 Li^+ ions could be intercalated during the following discharges with an average voltage around 3.2 V. These data correspond to 100 mA h g^{-1} and 80 mA h g^{-1} discharge capacities. In the tests as positive electrode *versus* Na/Na^+, this compound showed weak electrochemical activity in the 4.3–1.5 V range. Samples with smaller particle size would show better results and, to improve their performance, nanomaterials are certainly required.

The $Li_{0.5}Na_{0.5}MnFe_2(PO_4)_3$ and $Li_{0.75}Na_{0.25}MnFe_2(PO_4)_3$ compounds have also been synthesized by the group of Delmas *et al.* and their electrochemical activity *versus* Li has been tested, but none of them showed better specific capacity than that of the $NaMnFe_2(PO_4)_3$ phase.[61]

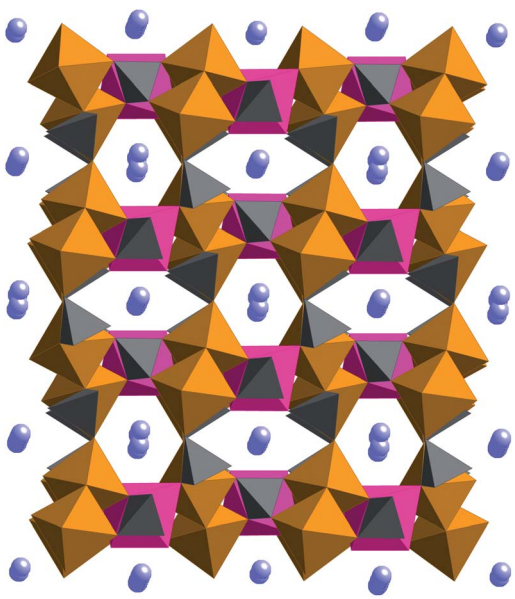

Fig. 22 View of the alluaudite structure in the *ab* plane.

3. Electrolytes

In recent times, the use of sodium complexed electrolyte films has been found to exhibit several advantages over their lithium counterparts. There are a few studies based on conductive polymeric electrolytes that have been completed for Na-ion batteries, in contrast to polymer electrolytes for Li-ion batteries.[62] The research and development on new electrolytes could be the key point for Na^+ battery success because they could avoid dendrite formation or interface aging, for instance. It is, therefore, a need to develop high sodium ion conducting non-aqueous electrolytes suitable for the fabrication of rechargeable sodium batteries. Sodium salts are often less soluble in organic solvents than the lithium analogs, which limits the choice of electrolytes. The development of sodium ion conducting nonaqueous polymer electrolytes should be preferred in view of their higher conductivity values (comparable to liquid electrolytes), mechanical and electrochemical properties.

However, it has been recently shown that the polymer electrolytes can be considered as an excellent substitute for the liquid electrolytes, due to their most appealing feature of free standing consistency which contributes easy handling and cell design, modularity and reliability in various electrochemical devices[63–65] (Fig. 23).

3.1. Gel polymer electrolytes for Na ion batteries

Several kinds of electrolytes comprising a high dielectric constant plasticizer or solvent or its solution with different salts

Fig. 23 Image of a NaTf/EMITf/PVdF-HFP gel polymer electrolyte film (from ref. 71). Reprinted from: D. Kumar and S. A. Hashmi, Ionic liquid based sodium ion conducting gel polymer electrolytes, *Solid State Ionics*, **181**, 416–423, Copyright 2010, with permission from Elsevier.

immobilized with the matrix of polymer hosts such as polyethylene oxide (PEO),[66,67] polyvinyl alcohol (PVA),[68] *etc.* have been reported. The solvent or salt-solution is retained in polymeric gel electrolyte and helps in the ionic conduction process, whereas the host polymer matrix provides mechanical stability by enhancing the viscosity of the gel electrolytes. An effective method is polymer blending because it reduces the crystalline content and enhances the amorphous content. So, Kumar *et al.* have obtained polymer blend electrolytes with great ionic diffusivity, based on polyethylene oxide and polyvinyl pyrrolidone complexed with NaF salt using the solution casting technique.[69]

In gel polymer electrolytes, the connected network of amorphous regions provides an improvement in ion mobility, and hence, ionic conductivity (Fig. 24). However, the properties of gel polymer electrolytes deteriorate over time due to loss of liquid. A possible remedy for prevention of deterioration in materials properties could to be replace low viscosity solvents with very high viscosity solvents. Thus, Patel *et al.* reported the benefits of introducing succinonitrile (a viscous organic plastic as additive) in PEO-$NaCF_3SO_3$ electrolytes. The addition of succinonitrile resulted in a rise of ionic conductivity and mechanical properties.[70]

Most of the reported gel polymer electrolytes comprise solvents such as propylene carbonate (PC), or ethylene carbonate (EC), but room temperature ionic liquids could also act as solvents to obtain thermally and electrochemically stable gel polymer electrolytes. Ionic liquids meet the requirements of plasticizing salts and also offer improved thermal and mechanical properties to flexible polymers. Innovative sodium salts or mixing salts (NaTFSI, NaFSI, NaTf…) could be used in these solvents. A new sodium ion conducting gel polymer electrolyte based on the solution of sodium triflate ($NaCF_3SO_3$) in ionic liquid EMI-triflate immobilized with the host polymer PVdF-HFP has been recently reported by Kumar and Hashmi (see ref. 71). This gel polymer electrolyte showed high ionic conductivity at room temperature with a sufficiently wide electrochemical potential window and excellent thermal stability (Fig. 25).

On the other hand, various research groups have reported composite/nanocomposite gel polymer electrolytes generated by the addition of the dispersion of micro- or nano-sized ceramic fillers. Bhide and Hariharan obtained a new Na^+ ion conducting polymer electrolyte $(PEO)_6$:$NaPO_3$ dispersed with 3–10 wt% $BaTiO_3$ fillers.[72] Aravindan *et al.* prepared sodium ion conducting composite polymer electrolytes by a solution casting technique in the skeleton of poly(vinylidene fluoride-*co*-hexafluoropropylene)/poly(ethyl methacrylate) (PVdF-HFP/PEMA) blend, with DC and EC as plasticizer and nanosized Sb_2O_3 as filler.[73] Finally, Kumar and Hashmi obtained gel polymer electrolyte nanocomposites based on poly(methylmethacrylate) (PMMA) and dispersed silica nanoparticles as fillers.[74] Such fillers generate a slight enhancement in the sodium ion transport number and preserve a porous structure that maximizes the adsorption of liquid electrolyte and reduces the risk of leakage. The enhancement in ionic conductivity due to addition of filler

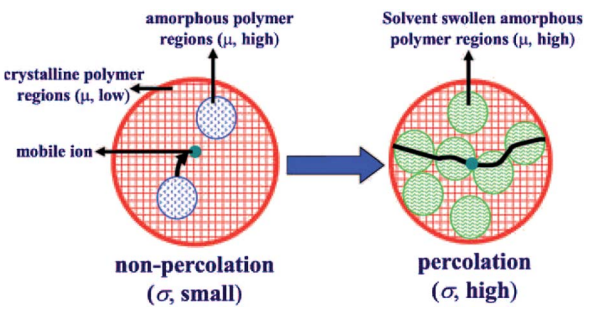

Fig. 24 Transformation of polymer electrolytes from non-percolative regions to a percolative region of gel electrolyte. Reprinted from: M. Patel, K. G. Chandrappa and A. J. Bhattacharyya, Increasing ionic conductivity of polymer–sodium salt complex by addition of a non-ionic plastic crystal, *Solid State Ionics*, **181**, 844–848, Copyright 2010, with permission from Elsevier.

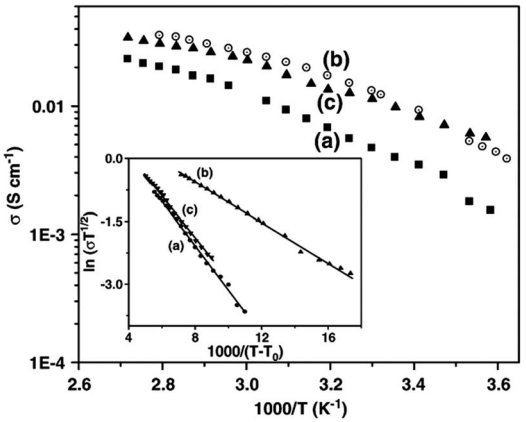

Fig. 25 Ionic conductivity as a function of temperature for the blends of ionic liquid/PVdF-HFP (a) 3 : 1 w/w; (b) 4 : 1 w/w; and (c) ionic liquid/PVdF-HFP (1 : 1 w/w) + NaTf gel polymer electrolyte. Reprinted from: D. Kumar and S. A. Hashmi, Ionic liquid based sodium ion conducting gel polymer electrolytes, *Solid State Ionics*, **181**, 416–423, Copyright 2010, with permission from Elsevier.

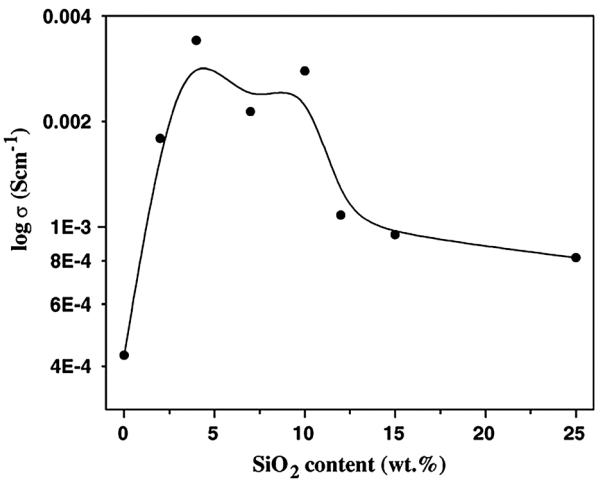

Fig. 26 Variation of room temperature electrical conductivity of gel polymer electrolyte nanocomposite films as a function of nano-sized SiO_2 content. Reprinted from: D. Kumar and S. A. Hashmi, Ion transport and ion–filler–polymer interaction in poly(methyl methacrylate)-based, sodium ion conducting, gel polymer electrolytes dispersed with silica nanoparticles, *Journal of Power Sources*, **195**, 5101–5108, Copyright 2010, with permission from Elsevier.

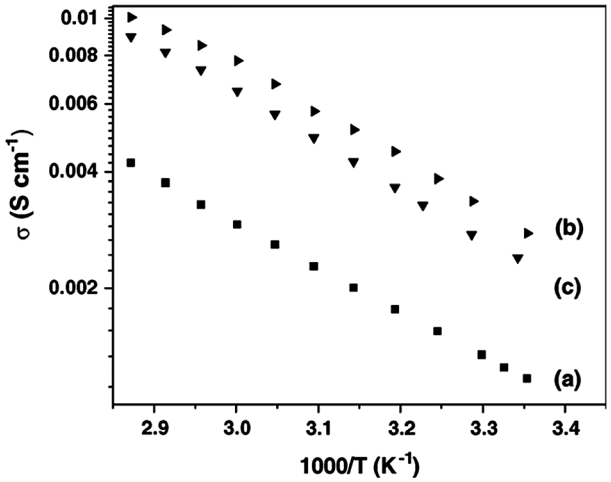

Fig. 27 Temperature dependence of electrical conductivity of (a) EC–PC–$NaClO_4$ + PMMA gel polymer electrolyte and with nano-SiO_2 of (b) 10 wt% and (c) 25 wt%. Reprinted from: D. Kumar and S. A. Hashmi, Ion transport and ion–filler–polymer interaction in poly(methyl methacrylate)-based, sodium ion conducting, gel polymer electrolytes dispersed with silica nanoparticles, *Journal of Power Sources*, **195**, 5101–5108, Copyright 2010, with permission from Elsevier.

particles depends on the filler concentration and amorphous phase in the polymer host matrix (Fig. 26 and 27).

Thakur *et al.* observed by FTIR spectroscopy the existence of ion pairs and free anions whose proportion varies due to the dispersion of filler particles. Furthermore, they proposed a mechanism based on ion–polymer, ion–ion, ion–filler and polymer–filler interactions along with the cluster formation at higher concentration of filler particles, which explains the variation of T_g with respect to filler concentration[75] (Fig. 28).

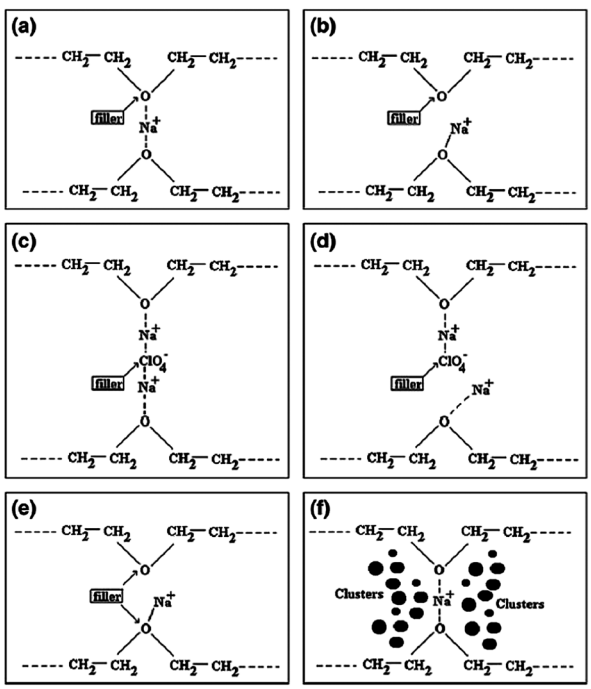

Fig. 28 Schema of ion–polymer matrix–filler interactions and cluster formation in the PEO matrix. Reprinted from: A. K. Thakur and S. A. Hashmi, Polymer matrix–filler interaction mechanism for modified ion transport and glass transition temperature in the polymer electrolyte composites, *Solid State Ionics*, **181**, 1270–1278, Copyright 2010, with permission from Elsevier.

3.2. Ceramic electrolytes for Na-ion batteries

Ceramic solid materials would be another kind of electrolytes for Na ion batteries. The use of a solid electrolyte would eliminate the need for a separator, and avoid the use of organic electrolytes, leading to safer batteries and avoiding leakage risks. Moreover, ceramic materials could facilitate miniaturization and make battery design more versatile.[76]

Among the possible ceramic materials, sodium β″-alumina solid electrolyte (BASE) ceramic and NASICON phases stand out as possible electrolytes in Na ion batteries. With respect to the Na-β alumina, there are two distinct crystal structures: β-Al_2O_3 (hexagonal: $P6_3/mmc$; $a_0 = 0.559$, $c_0 = 2.261$ mm) and β″-Al_2O_3 (rhombohedral: $R3m$; $a_0 = 0.560$, $c_0 = 3.395$ mm). They differ in chemical stoichiometry and the stacking sequence of oxygen ion across the conduction layer. In terms of conductivity at room temperature, single crystals can reach 0.1 S cm^{-1}. The ionic conductivity at 300 °C of a single crystal β″-Al_2O_3 is about 1 S cm^{-1}, which is almost 5 times that for polycrystalline β″-Al_2O_3 (0.2–0.4 S cm^{-1}). The β″-Al_2O_3 phase was found to give a better ionic conductivity than the β-Al_2O_3 phase. Nevertheless, it is difficult to obtain a uniform product because the synthesized β″-Al_2O_3 is often mixed with β-Al_2O_3 and with remnant $NaAlO_2$ distributed along grain boundaries. Besides its composition, the ionic conductivity of polycrystalline β″-Al_2O_3 depends on the ratio of β″/β and the microstructure (grain size, porosity, impurities, *etc.*). The strength and fracture toughness can be enhanced by incorporating ZrO_2 into the β″/β-Al_2O_3 matrix. It must be noted, however, that adding ZrO_2 into the β″-Al_2O_3 might deteriorate the electrical performance because ZrO_2 is not a sodium-ionic conductor at battery operating temperatures (<450 °C). However, the resistivity remains less than 10 Ω cm at 300 °C with up to 15 vol% of ZrO_2 addition. The enrichment in sodium or substitution of aluminium ions with mono- or divalent ions (*e.g.*, Li^+, Mg^{2+}) leads to higher Na^+ conductivity. Two ideal β″-Al_2O_3 stoichiometries, $Na_{1.67}Al_{10.33}Mg_{0.67}O_{17}$ (Mg^{2+} doped) and $Na_{1.67}Al_{10.33}Li_{0.33}O_{17}$ (Li^{2+} doped),[77] have been obtained but no conductivity values have been published.

On the other hand, NASICON phases stand for a well known family of Na^+ superionic conductors based on the formula $A_nM_2(XO_4)_3$ (A = alkali, M = transition metal, X = Si^{4+}, P^{5+}, S^{6+}, Mo^{6+}, *etc.*). More specifically, the compounds of general formula $Na_{1+x}Zr_2Si_xP_{3-x}O_{12}$ ($0 < x < 3$) were firstly suggested as solid electrolyte materials for Na^+ ion-based batteries,[78] and also proposed for all-solid-state electrochemical cells such as gas sensors,[79] ion sensors[80,81] and Na–S batteries.[82] The framework of these latter compounds is a phosphosilicate; thus, $Na_3Zr_2Si_2PO_{12}$ has corner sharing tetrahedra of phosphate and silicate with zirconia centered octahedral sites, where for every two octahedral sites there are three tetrahedral sites comprising two silicate and one phosphate center. This arrangement is repeated spatially to form the monoclinic/rhombohedral phase of NASICON.

The relationship between microstructure and electrical properties of the $Na_{1+x}Zr_2Si_xP_{3-x}O_{12}$ materials has been studied by Fuentes *et al.*[83] This work proved that grain size of NASICON yttria-doped tetragonal polycrystalline zirconia $(ZrO_2)_{0.97}(Y_2O_3)_{0.03}$ ceramics depends on sintering conditions, temperature and time. It showed an increase of the grain size when ceramics are sintered at higher temperatures or for longer periods of time. A maximum conductivity value of about 2.7×10^{-3} S cm^{-1} at room temperature was obtained with the yttria-doped tetragonal phase.

NASICON compounds have usually been synthesized by two methods: traditional ceramic route and sol–gel process (see ref. 78), but other synthetic strategies have also been used.[84–87]

Porkodi *et al.* have proposed a new synthesis method for these phases based on a molecular precursor.[88] The conductivity value of the best sample was 2.2×10^{-3} S cm^{-1}. Mixtures of $Na_4Zr_2Si_3O_{12}$ and TiO_2 have been patented by Takeuchi *et al.* as possible solid electrolytes for sodium–sulfur batteries,[89] but due to their conductivity value (4.9×10^{-4} S cm^{-1} at room temperature), they could also be tested as solid electrolytes for Na-ion technology.

Thin film solid electrolyte materials are very promising in the field of microbatteries. The relatively low conductivity of ionic conductors at room temperature can be optimized by using thin ionic conducting films, which improve ionic diffusion.[90] For this purpose, several processes have been used, such as RF sputtering,[91] laser ablation (see ref. 90), pulsed laser deposition[92] and spin coating methods.[80]

4. Anodic materials

The search for appropriate anodes for Na-ion batteries is complex, and, although a great variety of phases that can potentially be used as positive electrodes have been identified, very few materials have been reported to be useful as negative electrodes.

First, it must be stated that the use of metallic sodium is not advisable because of dendrite formation, as for metallic lithium. Besides, safety of sodium anodes has been further put into question by its low melting point of 97.7 °C compared to 180.5 °C for lithium.[93]

4.1. Carbon based-anodes

Although reversible electrochemical mechanism of lithium insertion in graphite for electrode in lithium ion batteries has been widely studied, most of the intercalation methods of alkali metals in graphite like vapor-phase reaction, high pressure reaction, electrochemical reaction and reaction in a solvent have rendered a much lower amount of Na ions between the graphene layers than for Li ions. This is due to the fact that sodium hardly forms staged intercalation compounds with graphite.[94] Besides this fact, graphite electrochemical insertion of sodium into graphite is expected to occur below the sodium plating potential (≤0.1 V), thus the reductive or charging process cannot be observed. However, for disordered carbons, insertion of sodium occurs at higher voltage than graphite and can be studied.

Doeff *et al.* studied the electrochemical insertion of sodium into a petroleum-coke carbon, observing a reversible capacity of

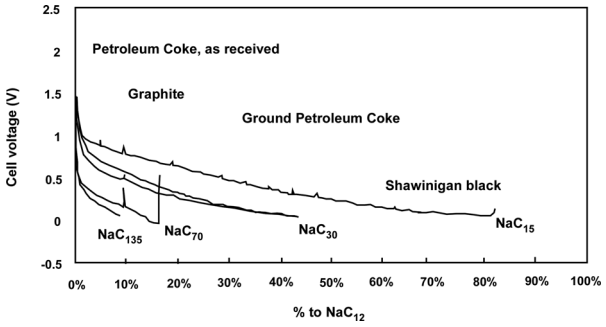

Fig. 29 Discharge curves (50 μA cm^{-2}) of Na/P(EO)$_8$NaCF$_3$SO$_3$/C cells heated to 86 °C. The spikes in the profiles are due to periodic current interrupts to assess the cell polarization. Reproduced by permission of The Electrochemical Society from ref. 11.

85 mA h g^{-1}. Thus, they evidenced the highest value reported for electrochemical "intercalation" of Na ion on carbonaceous materials (NaC_{15}) by using submicron particle sized carbon powder (see ref. 11) (Fig. 29). In this work, the authors also claimed that a stoichiometry of NaC_{24} (using coke) exhibited a reversible intercalation and also that by using crystalline graphite the final stoichiometry was NaC_{70}.

Tirado's group showed the reversible insertion of 0.0155 moles of Na per cm^3 of amorphous carbon black[95] and capacity values of 121 mA h g^{-1}, and 200 mA h g^{-1} considering only the discharge. It was observed that Na was stored between the bent graphene layers in the amorphous carbon black and that the carbon surface available was also the limiting factor for the capacity. The same research group, some years later, showed improvements by using amorphous carbon obtained from the pyrolysis of a polymeric resin forming microspheres with high surface area (Fig. 30).[96] The capacity value for reversible insertion of Na ion in this material was 285 mA h g^{-1} when ether type solvents were added to the liquid electrolyte. As ether-type solvents have shown higher chemical stability against metallic sodium than carbonate based-electrolytes, the optimization of liquid and solid electrolytes containing ether groups could also be the key to improve the electrochemical efficiency.

Dahn's group reported high gravimetric capacity values of 300 mA h g^{-1} for Na insertion by using hard carbons obtained from pyrolyzed glucose.[97] These values were close to those

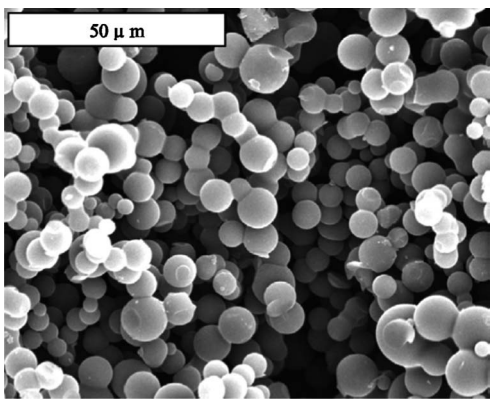

Fig. 30 SEM of carbon microspheres. Reproduced by permission of The Electrochemical Society from ref. 96.

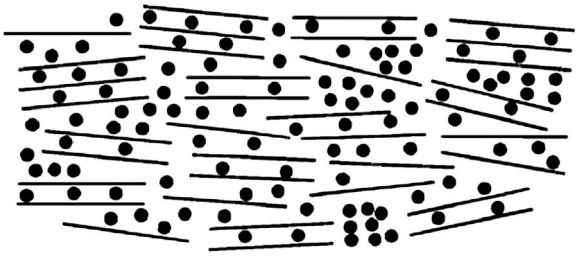

Fig. 31 "House of cards" model for sodium/lithium filled hard carbon. Reproduced by permission of The Electrochemical Society from ref. 97.

obtained for Li insertion in the same type of carbons. The voltage curves indicated that the insertion of alkali ions on hard carbon took place between the graphene layers of the graphitic particles and also into the pores created during the synthesis of this type of carbon (see Fig. 31).

Recently, Prof. Janek's group has prepared a templated carbon that showed 130, 120 and 100 mA h g^{-1} at *C*/5, 2*C* and 5*C* rates, respectively.[98] The first capacity value corresponds to a NaC_{17} nominal composition, that is, 17 carbon atoms are needed to accommodate one sodium atom. To date, similar capacities at room temperature could only be achieved for carbon black at currents as small as *C*/75 with very low cyclability. This remarkable result is attributed to the hierarchical pore system in the material, which consists of interconnected pores in the macro- and mesopore range that enable fast ion transport and short diffusion lengths. This structure is produced from porous silica as template and mesophase pitch as carbon precursor, which develops into a well-defined and thus highly conductive carbon microstructure compared to other carbons.

As it has been evidenced graphite did not allow significant sodium insertion whereas pyrolyzed enriched carbon precursors provided promising results. Other strategies can be adopted to enhance the accommodation of sodium ions in carbon materials. For instance, a grinding process raised the reversible capacity from 16 mA h g^{-1} to 187 mA h g^{-1} in graphite samples.[99] Sodium insertion enhancement can also be achieved with heteroatoms like hydrogen and oxygen after pyrolysis of cellulose to produce hard-carbons for intercalation. This method has evidenced higher reversible capacities for sodium intercalation than outgassed samples.[100]

4.2. Other anode materials

A recent communication by Palacín *et al.* describes the use of titanates as possible anodes for a room temperature Na-ion cell.[101] In this article, the $Na_2Ti_3O_7$ material is prepared and tested *versus* a sodium anode. This compound allows the intercalation of two sodium ions in a *plateau* around 0.3 V *vs.* Na/Na^+, which corresponds to a 200 mA h g^{-1} specific capacity. In this sense, other titanate compounds that have been tested in Li-ion cells, such as $Na_2Ti_6O_{13}$ or $Na_4Ti_5O_{12}$, could be applied to sodium ion technology. This way, a new family of compounds has joined the quest of an anode material for Na-ion cells.

Apart from carbonaceous materials, anodic compounds compatible with water-based electrolytes should be searched. Aqueous systems possess three big advantages against non-aqueous systems. First, they are nonflammable; second, materials and process costs are considerably reduced; and, third, aqueous solutions present high conductivity, thus leading to very low internal resistance.

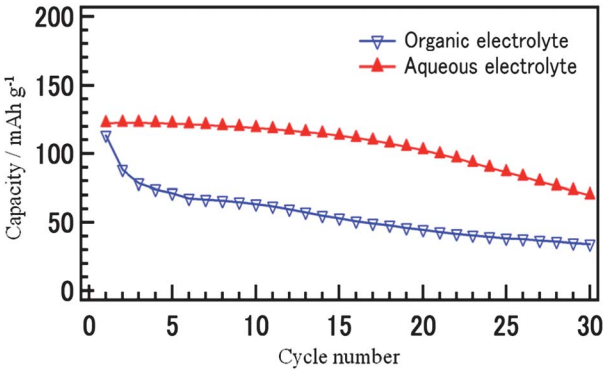

Fig. 32 Comparison of cyclability of $NaTi_2(PO_4)_3$ phase in an organic electrolyte of 1 M $NaClO_4$/EC : DMC (1 : 1) in volume, and aqueous electrolyte with 2 M Na_2SO_4 at a rate of 2.0 mA cm^{-2}. Reproduced by permission of The Electrochemical Society from ref. 102

Titanium phosphate has been recently reported as a good anode material to be used in aqueous Na-ion batteries.[102] The NASICON structure of $NaTi_2(PO_4)_3$ material can deliver a theoretical specific capacity of 130 mA h g^{-1}. This compound discharged at specific capacities of 120 and 123 mA h g^{-1} in non-aqueous and aqueous electrolytes, respectively. The aqueous electrochemical cell showed much lower polarization, better cyclability and rate capability. This way, in spite of the limited voltage range that is allowed to aqueous electrolytes, water-based cells would benefit from long cycle life, very low polarization, low cost and sustainability (Fig. 32).

5. Conclusions

Na-ion battery technology is a promising system as a substitute for Li-ion batteries for low cost applications due to the lower price and abundance of sodium, and its similar intercalation chemistry to lithium. There is much work to do in order to make Na-ion technology keep up with the standards needed for its application in, for example, grid storage. Several Na insertion cathodic materials have been studied: oxides, fluorophosphates and phosphates. Among them, oxides do not seem to be the best option due to the complexity of their insertion–extraction behavior that corresponds to multiple sloping electrochemical curves. On the other hand, phosphates and fluorophosphates can be a good choice because of their great stability and because greater working potentials are produced by the inductive effect of the phosphate polyanion. But these latter must be studied deeper in order to clarify their structural characteristics and Na insertion–extraction mechanisms.

In the field of ceramic electrolytes, sodium β″-alumina solid electrolyte (BASE) and NASICON materials such as sodium phosphosilicates exhibit major advantages because of their safe operation, versatility and no leakage. These materials also show promising ionic conductivity at room temperature. Single crystal β″-Al_2O_3 was reported to have a Na^+ conductivity of about 0.1 S cm^{-1} at room temperature. Meanwhile, NASICON type materials present about 10^{-4} to 10^{-3} S cm^{-1}. Therefore, BASE and

NASICON ceramic solid systems can be considered as alternative electrolytes for Na-ion batteries. On the other hand, gel polymer electrolytes with polymer blends or plastic crystalline as well as ionic liquids or nanosized ceramic fillers have been adequately demonstrated as a viable alternative to non-aqueous liquid electrolytes in electrochemical applications such as Na-ion batteries. The ambient temperature ionic conductivity in general is high ($\sim 10^{-4}$ to 10^{-3} Ω^{-1} cm^{-1}) and if suitably optimized may attain values similar to commercial non-aqueous liquid electrolytes ($\sim 10^{-2}$ Ω^{-1} cm^{-1}).

Further work must be done on graphitic-like materials as negative electrodes in Na based batteries. The chemical modification through the incorporation to the sp^2 structure of graphene sheets of heteroatoms during the synthesis or post-synthesis process could benefit the insertion of Na ions between the stacked layers of graphene.

The search for new anodes for Na-ion batteries is not restricted to carbonaceous materials. Other compounds, such as titanates, have recently been pointed out as new negative electrodes for these systems, and surely new phases will arise in order to play the counterpart for the great variety of cathode materials that have been researched up till now.

Acknowledgements

This work was financially supported by the Ministerio de Educación y Ciencia (MAT2010-19442), the Gobierno Vasco/Eusko Jaurlaritza (GIU06-11, ETORTEK CIC ENERGIGUNE 10, SAIOTEK SA-2010/00096 TEMAGEAL). V.P. thanks UPV/EHU for a postdoctoral fellowship.

Notes and references

1 B. L. Ellis, W. R. M. Makahnouk, Y. Makimura, K. Toghill and L. F. Nazar, *Nat. Mater.*, 2007, **6**, 749–753.
2 C. Wadia, P. Albertus and V. Srinivasan, *J. Power Sources*, 2011, **196**, 1593–1598.
3 B. L. Ellis, W. R. M. Makahnouk, W. N. Rowan-Weetaluktuk, D. H. Ryan and L. F. Nazar, *Chem. Mater.*, 2010, **22**, 1059–1070.
4 http://www.icispricing.com/il_shared/Samples/SubPage63.asp.
5 S. P. Ong, V. L. Chevrier, G. Hautier, A. Jain, C. Moore, S. Kim, X. Ma and G. Ceder, *Energy Environ. Sci.*, 2011, **4**, 3680–3688.
6 J. Braconnier, C. Delmas, C. Fouassier and P. Hagenmuller, *Mater. Res. Bull.*, 1980, **15**, 1797–1804.
7 S. Kikkawa, S. Miyazaki and M. Koizumi, *J. Power Sources*, 1985, **14**, 231–234.
8 J. Tarascon, *Solid State Ionics*, 1986, **22**, 85–96.
9 C. Fouassier, G. Matejka, J. Reau and P. Hagenmuller, *J. Solid State Chem.*, 1973, **6**, 532–537.
10 L. W. Shacklette, *J. Electrochem. Soc.*, 1988, **135**, 2669–2674.
11 M. M. Doeff, Y. Ma, S. J. Visco and L. C. De Jonghe, *J. Electrochem. Soc.*, 1993, **140**, L169–L170.
12 R. Berthelot, D. Carlier and C. Delmas, *Nat. Mater.*, 2010, **10**, 74–80.
13 Z. Lu and J. R. Dahn, *J. Electrochem. Soc.*, 2001, **148**, A1225–A1229.
14 M. M. Doeff, T. J. Richardson and L. Kepley, *J. Electrochem. Soc.*, 1996, **143**, 2507–2516.
15 M. M. Thackeray, *Prog. Solid State Chem.*, 1997, **25**, 1–71.
16 M. M. Doeff, M. Y. Peng, Y. Ma and L. C. De Jonghe, *J. Electrochem. Soc.*, 1994, **141**, L145–L147.
17 F. Sauvage, L. Laffont, J.-M. Tarascon and E. Baudrin, *Inorg. Chem.*, 2007, **46**, 3289–3294.
18 A. D. Tevar and J. F. Whitacre, *J. Electrochem. Soc.*, 2010, **157**, A870–A875.
19 J. F. Whitacre, A. Tevar and S. Sharma, *Electrochem. Commun.*, 2010, **12**, 463–466.
20 H. Liu, H. Zhou, L. Chen, Z. Tang and W. Yang, *J. Power Sources*, 2011, **196**, 814–819.
21 H. Liu, Y. Wang, L. Li, K. Wang, E. Hosono and H. Zhou, *J. Mater. Chem.*, 2009, **19**, 7885–7891.
22 T. Yamauchi, Y. Ueda and N. Môri, *Phys. Rev. Lett.*, 2002, **89**, 057002.
23 C. Presura, M. Popinciuc, P. van Loosdrecht, D. van der Marel, M. Mostovoy, T. Yamauchi and Y. Ueda, *Phys. Rev. Lett.*, 2003, **90**, 026402.
24 I. D. Gocheva, M. Nishijima, T. Doi, S. Okada, J.-I. Yamaki and T. Nishida, *J. Power Sources*, 2009, **187**, 247–252.
25 Y. Yamada, T. Doi, I. Tanaka, S. Okada and J.-I. Yamaki, *J. Power Sources*, 2011, **196**, 4837–4841.
26 A. Yamada, S. C. Chung and K. Hinokuma, *J. Electrochem. Soc.*, 2001, **148**, A224.
27 C. Burba and R. Frech, *Spectrochim. Acta, Part A*, 2006, **65**, 44–50.
28 P. Moreau, D. Guyomard, J. Gaubicher and F. Boucher, *Chem. Mater.*, 2010, **22**, 4126–4128.
29 A. Wizansky, *J. Solid State Chem.*, 1989, **81**, 203–207.
30 K. Zaghib, J. Trottier, P. Hovington, F. Brochu, A. Guerfi, A. Mauger and C. M. Julien, *J. Power Sources*, 2011, **196**, 9612–9617.
31 C. Delacourt, J. Rodríguez-Carvajal, B. Schmitt, J.-M. Tarascon and C. Masquelier, *Solid State Sci.*, 2005, **7**, 1506–1516.
32 J. N. Reimers and J. R. Dahn, *J. Electrochem. Soc.*, 1992, **139**, 2091–2097.
33 J. Molenda, C. Delmas, P. Dordor and A. Stoklosa, *Solid State Ionics*, 1984, **12**, 473–477.
34 K. T. Lee, T. N. Ramesh, F. Nan, G. Botton and L. F. Nazar, *Chem. Mater.*, 2011, **23**, 3593–3600.
35 J. Barker, M. Y. Saidi and J. L. Swoyer, *Electrochem. Solid-State Lett.*, 2003, **6**, A1–A4.
36 J. Le Meins, *J. Solid State Chem.*, 1999, **148**, 260–277.
37 J. Zhao, J. He, X. Ding, J. Zhou, Y. Ma, S. Wu and R. Huang, *J. Power Sources*, 2010, **195**, 6854–6859.
38 J. Barker, M. Y. Saidi and J. L. Swoyer, *J. Electrochem. Soc.*, 2004, **151**, A1670–A1677.
39 H. Zhuo, X. Wang, A. Tang, Z. Liu, S. Gamboa and P. J. Sebastian, *J. Power Sources*, 2006, **160**, 698–703.
40 Z. Liu, X. Wang, Y. Wang, A. Tang, S. Yang and L. He, *Trans. Nonferrous Met. Soc. China*, 2008, **18**, 346–350.
41 W. Massa, O. Yakubovich and O. Dimitrova, *Solid State Sci.*, 2002, **4**, 495–501.
42 A. Tsirlin, R. Nath, A. Abakumov, Y. Furukawa, D. Johnston, M. Hemmida, H.-A. Krug von Nidda, A. Loidl, C. Geibel and H. Rosner, *Phys. Rev. B: Condens. Matter Mater. Phys.*, 2011, **84**, 014429.
43 F. Sauvage, E. Quarez, J. Tarascon and E. Baudrin, *Solid State Sci.*, 2006, **8**, 1215–1221.
44 R. Gover, A. Bryan, P. Burns and J. Barker, *Solid State Ionics*, 2006, **177**, 1495–1500.
45 J. Barker, R. K. B. Gover, P. Burns and A. J. Bryan, *Electrochem. Solid-State Lett.*, 2006, **9**, A190–A192.
46 T. Jiang, G. Chen, A. Li, C. Wang and Y. Wei, *J. Alloys Compd.*, 2009, **478**, 604–607.
47 N. Recham, J.-N. Chotard, L. Dupont, K. Djellab, M. Armand and J.-M. Tarascon, *J. Electrochem. Soc.*, 2009, **156**, A993–A999.
48 J. Wolfenstine and J. Allen, *J. Power Sources*, 2005, **142**, 389–390.
49 S. Okada, M. Ueno, Y. Uebou and J.-I. Yamaki, *J. Power Sources*, 2005, **146**, 565–569.
50 I. V. Zatovsky, *Acta Crystallogr., Sect. E: Struct. Rep. Online*, 2010, **66**, i12.
51 J. Gopalakrishnan and K. K. Rangan, *Chem. Mater.*, 1992, **4**, 745–747.
52 J. Gaubicher, C. Wurm, G. Goward, C. Masquelier and L. Nazar, *Chem. Mater.*, 2000, **12**, 3240–3242.
53 B. Cushing, *J. Solid State Chem.*, 2001, **162**, 176–181.
54 D. Morgan, G. Ceder, M. Y. Saidi, J. Barker, J. Swoyer, H. Huang and G. Adamson, *Chem. Mater.*, 2002, **14**, 4684–4693.
55 K. Yoshida, K. Toda, K. Uematsu and M. Sato, *Key Eng. Mater.*, 1999, **157–158**, 289–296.
56 Y. Uebou, T. Kiyabu, S. Okada and J.-I. Yamaki, *The Reports of Institute of Advanced Material Study*, Kyushu University, 2002, vol. 16, pp. 1–5.
57 A. Andersson, *Solid State Ionics*, 2001, **140**, 63–70.

58 L. S. Plashnitsa, E. Kobayashi, Y. Noguchi, S. Okada and J.-I. Yamaki, *J. Electrochem. Soc.*, 2010, **157**, A536–A543.
59 T. J. Richardson, *J. Power Sources*, 2003, **119–121**, 262–265.
60 K. Trad, D. Carlier, L. Croguennec, A. Wattiaux, M. Ben Amara and C. Delmas, *Chem. Mater.*, 2010, **22**, 5554–5562.
61 K. Trad, D. Carlier, L. Croguennec, A. Wattiaux, M. Ben Amara and C. Delmas, *Inorg. Chem.*, 2010, **49**, 10378–10389.
62 J. W. Fergus, *J. Power Sources*, 2010, **195**, 4554–4569.
63 A. M. Stephan, *Eur. Polym. J.*, 2005, **41**, 15–21.
64 S. Hashmi, *Natl. Acad. Sci. Lett.*, 2004, **27**, 27–46.
65 J. B. Goodenough and Y. Kim, *Chem. Mater.*, 2010, **22**, 587–603.
66 S. R. Mohapatra, A. K. Thakur and R. N. P. Choudhary, *Ionics*, 2007, **14**, 255–262.
67 V. M. Mohan, V. Raja, P. B. Bhargav, A. K. Sharma and V. V. R. N. Rao, *J. Polym. Res.*, 2007, **14**, 283–290.
68 P. B. Bhargav, V. M. Mohan, A. K. Sharma and V. V. R. N. Rao, *Ionics*, 2007, **13**, 441–446.
69 K. Kiran Kumar, M. Ravi, Y. Pavani, S. Bhavani, A. K. Sharma and V. V. R. Narasimha Rao, *Phys. B*, 2011, **406**, 1706–1712.
70 M. Patel, K. G. Chandrappa and A. J. Bhattacharyya, *Solid State Ionics*, 2010, **181**, 844–848.
71 D. Kumar and S. A. Hashmi, *Solid State Ionics*, 2010, **181**, 416–423.
72 A. Bhide and K. Hariharan, *Polym. Int.*, 2008, **57**, 523–529.
73 V. Aravindan, C. Lakshmi and P. Vickraman, *Curr. Appl. Phys.*, 2009, **9**, 1106–1111.
74 D. Kumar and S. A. Hashmi, *J. Power Sources*, 2010, **195**, 5101–5108.
75 A. K. Thakur and S. A. Hashmi, *Solid State Ionics*, 2010, **181**, 1270–1278.
76 J. F. M. Oudenhoven, L. Baggetto and P. H. L. Notten, *Adv. Energy Mater.*, 2011, **1**, 10–33.
77 Z. Yanhg, J. Zhang, M. C. W. Kintner-Meyer, X. Lu, D. Choi and J. Lemmon, *Chem. Rev.*, 2011, **111**, 3577–3613.
78 R. O. Fuentes, F. M. Figueiredo, F. M. B. Marques and J. E. Franco, *Solid State Ionics*, 2001, **140**, 173–179.
79 S. Yao, Y. Shimizu, N. Miura and N. Yamazoe, *Chem. Lett.*, 1990, 2033–2036.
80 P. Fabry, J. P. Gros, J. F. Million-Brodaz and M. Kleitz, *Sens. Actuators*, 1988, **15**, 33–49.
81 P. Fabry, Y. L. Huang, A. Caneiro and G. Patrat, *Sens. Actuators, B*, 1992, **6**, 299–303.
82 Y. Shimizu, *Solid State Ionics*, 2000, **132**, 143–148.
83 R. O. Fuentes, F. Figueiredo, F. M. B. Marques and J. I. Franco, *Ionics*, 2002, **8**, 383–390.
84 M. L. Di Vona, E. Traversa and S. Licoccia, *Chem. Mater.*, 2001, **13**, 141–144.
85 A. Ignaszak, P. Pasierb, R. Gajerski and S. Komornicki, *Thermochim. Acta*, 2005, **426**, 7–14.
86 R. Fuentes, F. Figueiredo, M. Soares and F. Marques, *J. Eur. Ceram. Soc.*, 2005, **25**, 455–462.
87 P. R. Slater and C. Greaves, *J. Mater. Chem.*, 1994, **4**, 1463–1467.
88 P. Porkodi, V. Yegnaraman, P. Kamaraj, V. Kalyanavalli and D. Jeyakumar, *Chem. Mater.*, 2008, **20**, 6410–6419.
89 T. Takeuchi, E. Bétourne, M. Tabuchi, O. Nakamura and H. Kageyama, *US Pat.* 006117595A, 2000.
90 M. Morcrette, P. Barboux, A. Laurent and J. Perrière, *Solid State Ionics*, 1997, **93**, 283–290.
91 D. Ivanov, J. Currie, H. Bouchard, A. Lecours, J. Andrian, A. Yelon and S. Poulin, *Solid State Ionics*, 1994, **67**, 295–299.
92 R. Izquierdo, E. Quenneville, D. Trigylidas, F. Girard, M. Meunier, D. Ivanov, M. Paleologou and A. Yelon, *J. Electrochem. Soc.*, 1997, **144**, L323–L325.
93 V. L. Chevrier and G. Ceder, *J. Electrochem. Soc.*, 2011, **158**, A1011–A1014.
94 J. Sangster, *J. Phase Equilib. Diffus.*, 2007, **28**, 571–579.
95 R. Alcántara, J. M. Jiménez-Mateos, P. Lavela and J. L. Tirado, *Electrochem. Commun.*, 2001, **3**, 639–642.
96 R. Alcántara, P. Lavela, G. F. Ortiz and J. L. Tirado, *Electrochem. Solid-State Lett.*, 2005, **8**, A222–A225.
97 D. A. Stevens and J. R. Dahn, *J. Electrochem. Soc.*, 2000, **147**, 1271–1273.
98 S. Wenzel, T. Hara, J. Janek and P. Adelhelm, *Energy Environ. Sci.*, 2011, **4**, 3342–3345.
99 P. Thomas and D. Billaud, *Electrochim. Acta*, 2000, **46**, 39–47.
100 J. R. Dahn, T. Zheng, Y. Liu and J. S. Xue, *Science*, 1995, **270**, 590–593.
101 P. Senguttuvan, G. Rousse, V. Seznec, J.-M. Tarascon and M. R. Palacín, *Chem. Mater.*, 2011, **23**, 4109–4111.
102 S. I. Park, I. Gocheva, S. Okada and J.-I. Yamaki, *J. Electrochem. Soc.*, 2011, **158**, A1067–A1070.